João Manuel Duarte Ferreira

Modelling the Polymeric Profile
Extrusion Cooling Stage with OpenFOAM®

Modelling the Polymeric Profile
Extrusion Cooling Stage with OpenFOAM®

João Manuel Duarte Ferreira

UMinho | 2015

dezembro de 2015

Universidade do Minho
Escola de Engenharia

João Manuel Duarte Ferreira

Modelling the Polymeric Profile
Extrusion Cooling Stage with OpenFOAM®

Dissertação de Mestrado
Ciclo de Estudos Integrados Conducentes ao
Grau de Mestre em Engenharia de Polímeros

Trabalho efectuado sob a orientação do
Professor Doutor João Miguel Amorim Novais Costa
Nóbrega

dezembro de 2015

DECLARAÇÃO

Nome: João Manuel Duarte Ferreira

Endereço eletrónico: jmdf.ferreira@gmail.com   Telefone: +34698107329 / +351919717667

Bilhete de Identidade/Cartão do Cidadão: 139280995ZZ2

Título da dissertação: Modelling the Polymeric Profile Extrusion Cooling Stage with OpenFOAM®

Orientador:

Professor Doutor João Miguel Amorim Novais Costa Nóbrega

Ano de conclusão: 2015

Mestrado Integrado em Engenharia de Polímeros

É AUTORIZADA A REPRODUÇÃO PARCIAL DESTA DISSERTAÇÃO (indicar, caso tal seja necessário, nº máximo de páginas, ilustrações, gráficos, etc.), APENAS PARA EFEITOS DE INVESTIGAÇÃO, MEDIANTE DECLARAÇÃO ESCRITA DO INTERESSADO, QUE A TAL SE COMPROMETE.

Universidade do Minho, _____/_____/_____

Assinatura:

ACKNOWLEDGMENTS

During this journey of project development and writing this thesis, several persons were fundamental to accomplish my objectives.

Firstly, I would like to thank Professor João Miguel Amorim Novais Costa Nóbrega for all the guidance, corrections and knowledge inputs. Also, for all the opportunities I had access during this journey.

I also would like to thank to all the members of Gompute S. L. company, that provided crucial help throughout the development of this work.

Finally, I am forever thankful to my parents and my brother for all the support, help and guidance through these years.

ABSTRACT

Nowadays the importance of the Computational Fluid Dynamics in polymer processing applications is really high, since it can provide useful data that can be used to anticipate the behaviour of the system under study, when subjected different service conditions, and thus guide its design and/or optimization. There are different options available when choosing the platform to perform such studies, which can be mainly divided into commercial and the free/open source numerical codes. Besides the obvious differences in terms of cost, the first do not allow changes on the source code while the latter allows it. OpenFOAM® computational library is an example of a free and open source code that comprises several pre-programmed solvers, allows full customization by the user and provides a solid and consolidated base for the development of customized numerical tools.

The problem of interest integrated in the field of polymer processing, comprises the modelling of cooling and calibration of an extruded polymer profile with unstructured meshes. Numerical tools had to be created to fulfil the requirements and for that OpenFOAM® was used and modified.

To meet the modelling requirements the *cthMultiRegionFoam* solver, that solves momentum, energy and continuity equations, was modified to solve only the energy conservation equation since, at the profile extrusion calibration stage, the velocity field is known and constant on the entire domain. Different verifications were performed on the developed code, by comparing its predictions with, analytical solutions, for simple problems and with results available on the scientific literature, in order to evaluate its accuracy. Convergence order studies were performed using different meshes to evaluate the order of convergence and the calculation accuracy and to choose the best mesh refinement level to use on the subsequent studies. In order to evaluate the code capabilities, studies involving cooling and calibration of an extruded polymer profile using different layouts, process and geometrical parameters were also undertaken.

The developed code was tested under different verification problems and, the results obtained, allowed to assess it, for the cooling stage. Regarding conclusions, the studies made possible the evaluation of which process and geometrical parameters influence the most. This revealed that using several calibrators have advantages when compared to only use one, also that the profile velocity has the higher impact on the final results.

RESUMO

Hoje em dia, é grande a importância da Dinâmica de Fluídos Computacional nas aplicações de processamento de polímeros, a informação produzida por estes estudos possibilita a antecipação do comportamento que o sistema em estudo terá, quando sujeito a diferentes condições de serviço, e ajudar no desenho e otimização do mesmo. Existem diferentes opções disponíveis para a execução deste tipo de estudos, que podem ser divididas em códigos comercial e gratuito/aberto. À parte da diferença óbvia em termos de custo, o primeiro não possibilita a alteração do código fonte, enquanto o segundo o possibilita. OpenFOAM® é um exemplo de código aberto e gratuito, que contém diversos *solvers* pré-programados, possibilita a sua total modificação por parte do utilizador e apresenta-se como um base sólida e consolidada para o desenvolvimento de ferramentas numéricas personalizadas.

O problema de interesse integrado na área de processamento de polímeros, compreende a modelação da etapa de arrefecimento e calibração do processo de extrusão de perfil, utilizando malhas não estruturadas. Ferramentas numéricas tiveram de ser desenvolvidas para cumprir os requisitos de modelação e, para isso, o OpenFOAM® foi utilizado e modificado.

Para cumprir os requisitos de modelação o *solver chtMultiRegionFoam*, que resolve as equações de momento, conservação de energia e continuidade, foi modificado para apenas resolver a equação de conservação de energia, dado que na etapa de calibração da extrusão de perfil, o campo de velocidades é conhecido e constante em todo o domínio. Diferentes verificações foram realizadas com o código desenvolvido, comparando as suas previsões com soluções analíticas, para problemas simples e com resultados disponíveis na literatura científica, para avaliar a sua precisão. Estudos de ordem de convergência foram realizados com diferentes malhas para avaliar a convergência e a precisão de cálculo, de forma a também escolher o melhor refinamento de malha para os estudos a realizar. Para avaliar as capacidades do código, estudos envolvendo a etapa de arrefecimento e calibração da extrusão de perfil com diferentes *layouts*, parâmetros geométricos e de processo foram realizados.

O código desenvolvido foi testado sobre diferentes problemas de verificação e, com os resultados obtidos, possibilitou a sua aferição para a etapa de arrefecimento. Relativamente a conclusões, os estudos possibilitaram a avaliação de quais os parâmetros geométricos e de processo têm mais influencia. Isto relevou que a utilização de diversos calibradores tem vantagens à utilização de apenas um e também que a velocidade do perfil é o parâmetro com mais impacto nos resultados finais.

CONTENTS

LIST OF FIGURES

LIST OF TABLES

LIST OF ABBREVIATIONS AND ACRONYMS

OF - Open Source Field Operation and Manipulation, OpenFOAM®

CFD – Computational Fluid Dynamics

HPC – High Performance Computing

FEM – Finite Element Method

FVM – Finite Volume Method

1.   INTRODUCTION

1.1 Problem to be solved

The problem of interest in this work is the modelling of the cooling and calibration stage of a thermoplastic profile extrusion line. A profile extrusion line is typically composed by five stages, as illustrated in the Fig. 1, which can be described as follows:

    1) Extruder – At this stage the raw polymer pellets are melted, homogenized and conveyed, with the help of a screw, into the extrusion die;

    2) Die – The forming stage, where the polymer melt is progressively transformed from the circular cross section, at the extruder outlet, to a cross section similar to the profile to be produced;

    3) Calibration/Cooling – The polymer melt is cooled down, and also calibrated, until a sufficiently low temperature that guarantees its shape during the remaining stages of the extrusion line;

    4) Haul-off – This is a device that pulls the extrudate and is responsible for the maintenance of the extrusion linear velocity;

    5) Saw – At final stage of the process the extrudate is cut into smaller sections and stored;
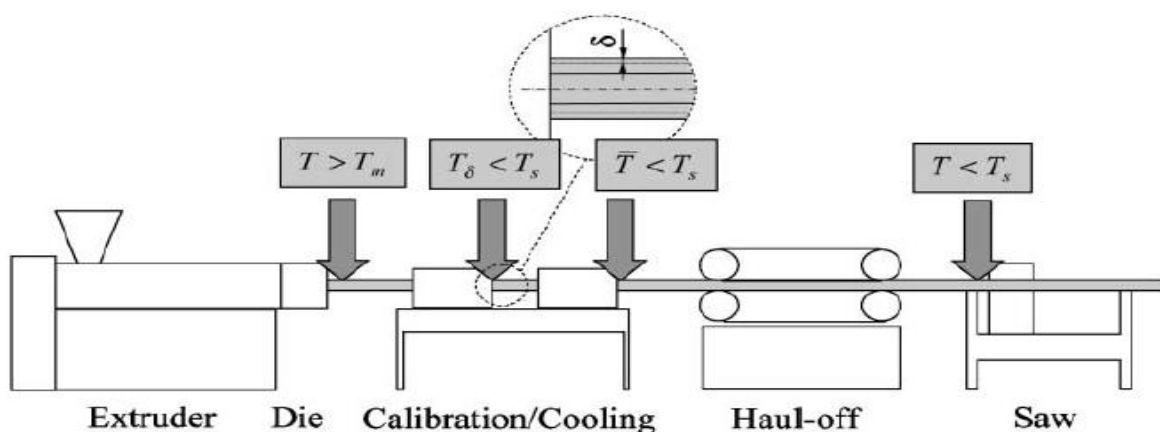
Fig. 1 - Typical extrusion line for the production of thermoplastic profiles, Nóbrega J. M. et al. (2004)

Due to the complex rheological behaviour of polymer melts, it is difficult to obtain a profile with the desire cross section after emerging from the extrusion die flow channel. Thus the third stage of the

process, is very important, not only to impose the profile main dimensions, but also to assure enough mechanical resistance to support the loads imposed at the downstream stages. Being a relevant stage for the extrusion process makes the numerical modelling of this stage quite relevant.

The numerical modelling of the calibration/cooling stage provides a high quantity of useful information that can be used to improve the system efficiency, leading to higher production rates or to achieve a more uniform cooling, relevant to minimize the level of induced thermal residual stresses. The reasons behind the modelling of this stage are the need to obtain the temperature distribution on the polymer profile. The more uniform temperature distribution along the profile the better and this can be obtained by adjusting the geometrical and process parameters on the calibrator, such adjustments can be performed considering the information retrieved from the numerical modelling studies. At the end, studying the influence of the parameters that can be controlled on this stage, it is possible to obtain the most efficient system layout.

The extrusion cooling stage comprises two main components (see Fig. 1). A polymeric profile, produced by extrusion, and a metal calibrator. The polymer profile travels at a constant and uniform velocity relatively to the calibrator, which is stationary. Regarding the calibrator, comprises a variable number of cooling channels, which are filled with a cooling fluid at low temperature that are used to remove energy from the system. Depending of the cooling requirements more than one calibrator can be used.

This stage has variables that can be changed or controlled. In terms to conceive a calibration system one must specify: the number of cooling units, their length and distance between them. Additionally, the variables of the process that can be controlled are: the cooling fluid temperature and the profile velocity. These are the main variables of the process that can be controlled and/or changed and that can be established with the support of numerical studies.

1.2 State of the art

The use of CFD on the polymer processing area is growing at a good rate, which is logic since the advantages of using numerical modelling tools, during the design stage, are immense. For areas like injection moulding, CFD is used frequently while to design parts and/or their processing tools, although on the extrusion process, CFD is not used so frequently, mainly due to the absence of adequate numerical tools, which is a clear limitation for the extrusion process development.

The first works available in the literature was the 2D FEM approach proposed by Menges et al. (1987), which was able to deal with any profile cross section but without considering axial heat fluxes. Later, an approach named Corrected Slice Method was proposed by Sheehy et al. (1994). This extends the 2D approach described by Menges et al. (1987), to take into account the axial heat fluxes within the system. The developed method allow the use of complex cross sections considering axial heat fluxes, although with the restrain of being an hybrid 2D model, which limits, in several ways, the extent of the studies that can be conducted. A more complex approach was handled by Nóbrega J. M. (2004), where numerical tools were developed to model this stage, and were coupled with automatic optimization approaches. In the same subject, another approach was proposed by Nóbrega J. M. et al. (2004) to model the thermal interchanges between the polymer profile and the calibrator. In this study the temperature distribution of the polymer profile when crossing this stage was obtained, allowing to predict the efficiency of the cooling system. Despite their obvious advantages, these numerical tools can only work with structured meshes which restrain, in a significant way, the complexity of the profile cross sections that can be studied.

It is important to understand that the development of numerical tools need a large amount of information about the specific situation intended to be modelled, such as the properties of the material that are being used on the model. Regarding the cooling and calibration stage of the extrusion process, the interface between the polymer and the calibrator is a critical area of the system, which requires special techniques to obtain the heat transfer coefficient, in order to correctly consider the heat exchange between both parts. The characterization of the heat transfer coefficient for the extrusion cooling system was conducted by Pittman J. F. T. et al. (1994) and Mousseay P. et al. (2009) where the contact resistance is evaluated. The first study is the most complete one, although this provides useful information just for thick pipe extrusion where the cooling is performed by immersion in water. This is not the usual approach on profile extrusion, where the cooling is performed by contact between the profile and the calibrator, which affects the heat transfer at the polymer-calibrator interface and creates problems related with friction. The second study allows the understanding of all the heat transfer phenomena occurring during the profile cooling stage, although the analysis were undertaken applying vacuum on both side of the plastic tape, which usually is not the case in practical extrusion. Both studies provide useful information, regarding the evaluation of the heat transfer coefficient on the polymer-calibrator interface, however the values obtained are for specific conditions. Recently, a prototype developed by Carneiro O. S. et al. (2013) to perform an evaluation of the heat transfer coefficient value on the interface polymer-calibrator, under the typical conditions used on the profile extrusion.

The information available in the scientific literature show that is possible to correctly model the cooling and calibration stage of the extrusion process and that there are tools already developed capable of modelling it, although, with some limitations. More versatile numerical codes, able to deal with realistic problems, which in general involve complex geometries, are needed. To be able to deal with more complex geometries, these numerical tools should be able to work with 3D unstructured meshes.

1.3 Objectives

The main objective of this work is to develop and verify numerical tools adequate to aid the design of the cooling and calibration stage of profile extrusion comprising complex problems.

Several smaller tasks have to be fulfilled to reach the main purpose stated above. At the initial part of the work a numerical code must be developed to meet the modelling requirements of the cooling stage of profile extrusion and also be able to deal with complex geometries, thus it should work with unstructured meshes. The second target of this work is the developed code verification. For this purpose, the developed code predictions should be compared with analytical results, for simple problems, with results provided in the literature. During the verification work, the order of convergence of the developed code should be also verified. It is also an objective of this work to perform systematic studies with a typical profile extrusion problem, to evaluate the developed code sensitivity and, in a qualitative manner, its predictions.

1.4 Thesis structure

The Section 1 briefly describes the polymer extrusion process and addresses the problem being solved in this project, as well as a state of the art, that summarizes the most relevant contributions on the area. The Section 2 presents the work undertaken to develop the numerical code, adequate for the problem of interest. The Section 3 comprises the code verification, which was done using two different case studies. Following, on Section 4, aiming to evaluate the sensitivity of the developed code, it was used to investigate, in detail, the cooling stage of a representative profile extrusion problem. The Section 5, and final one, presents the conclusions and outlook of the work done in this project.

2. NUMERICAL CODE

2.1 OpenFOAM Computational Library

Open Source Field Operation and Manipulation, abbreviated as OpenFOAM®, is a free and open source C++ numerical computational library. It is used primarily to create executables, known as *applications*, this category is then divided into two sub-categories which are *solvers,* routines used to solve continuum mechanics problems, using the Finite Volume Method (FVM), and *utilities* which are used to all types of data manipulation from pre-processing to post-processing. A large amount of *solvers* and *utilities* are available in each OF distribution, covering a large range of problems. Also OF has its own pre- and post-processing environments as well as the solving one, this means that the all main steps of a numerical study are done under OF's utilities which ensures correct data travel between the environments. Although the main strength of OF is that *solvers* and *utilities* can be created or modified by the users and then be used on a specific case, this requires some knowledge of the underlying method, physics and also programming techniques involved. Bottom line the OF provides a solid and verified base to produce numerical tools to solve specific problems, allowing the user to add desired features to *applications* or *utilities* or even remove some to obtain better performance.

As stated above one of the main advantages and capabilities of OF is the free and open source nature of the code, allowing to understand, from the user perspective, how the routines are performed and use them without any type of fee. Another main advantage is allowing the user to modify the source code of the already provided *applications* or *utilities* and also provide a solid base to make new *applications* or *utilities* without any kind of restrain, this opens a whole new level of possible developed work. The nature of the code also allows the users to exchange knowledge and creations which makes this library very community driven and a lot of improvements are inserted in every new version release. With this the number of *applications* is large making possible a huge amount of different CFD studies using this library.

The need to develop numerical tools to solve the problem addressed in this project made OF a seriously interesting base to work. In fact, OF has a solver that almost meets all the requirements to solve the problem of interest, although a few changes on it were needed to make it suit the modelling requirements. Also, the OF is booming in several CFD areas, although there are just a few studies on the

polymer extrusion, then here OF is going to be tested to model the extrusion process calibration and cooling stage. The capability of OF to efficiently work in an HPC environment is also a good reason to work with it in this project, since an HPC platform was available to perform the studies. Using this HPC platform, that provides a higher amount of resources, it reduces the calculation time as well as allow the use of bigger meshes.

2.2 Solver chtMultiRegionFoam

The OF *chtMultiRegionFoam* is a solver developed for conjugate heat transfer between solid and fluid regions. The differences between the type of regions, considered by the solver, are that a solid region is stationary, where the energy conservation equation is solved, and a fluid region has a velocity field, where the linear momentum, energy conservation and continuity equations are solved. The solvers flowchart is illustrated in Fig. 2.
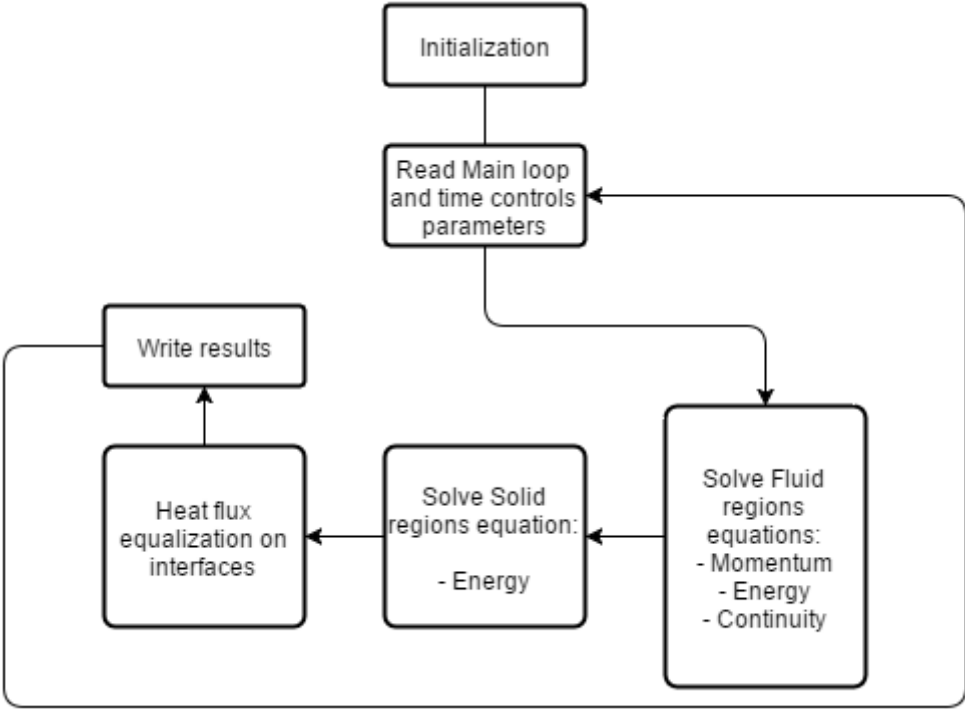
Fig. 2 - Flowchart of chtMultiRegionFoam solver steps

The solver performs several steps during, which can be described as follows:

1) Initialization – This step starts by initializing the turbulence, radiation and thermodynamic models and the time variables. Then it continues with the definition of the solid and fluid regions on the mesh, finalizing with the creation of the fields present in each region like velocity, pressure and temperature;

2) Read Main loop and time controls parameters – In this step the solver reads the control parameters that are used by the Main loop algorithm and by the solver;

3) Solve Fluid regions equations – For each fluid region the momentum, energy conservation and continuity equations are solved;

4) Solve Solid regions equations – For each solid region the energy conservation equation is solved;

5) Heat flux equalization on interfaces – In this step the heat flux is calculated on the interfaces in preparation for the next time step to account the heat transfer between different regions;

6) Write results – the results obtained by solving the fluid and solid regions equations are written and the solver goes back to the step 2 to solve the equations for the next time step;

Analysing the model requirements, as described on the Section 1.1, and the potential of *chtMultiRegionFoam* it can be concluded that this solver can be used to solve the problem being addressed in this project. With the capability of solving the equations on two or more different regions, with different properties but connected by one or more boundaries, makes it a good choice, when dealing with a model that has at least two different regions, polymer and calibrator.

2.3 Numerical Procedure

The model being developed here requires that only the energy conservation equation needs to be solved to obtain the thermal field on the calibrator (2) and polymeric profile (1) regions. This happens because the velocity field on the profile is known and also constant throughout the entire domain, which makes the energy conservation equation the only one that has to be solved. As described by Nóbrega J. M. et al. (2004), the energy conservation equation can written as follows for the polymeric profile:

$$\nabla \cdot \left(\rho c_p \vec{u} T \right) - \frac{k}{\rho c_p} \nabla^2 T = 0 \tag{1}$$

and for the calibrator:

$$\frac{k}{\rho c_p} \nabla^2 T = 0 \tag{2}$$

The polymer region have two different transport mechanism, which are the advection and diffusion. For the calibrator region, where the velocity field is null, which makes the only transport mechanism existent in this region be the diffusion.

The system to model two different regions where the equations described above are solved. To account the heat fluxes exchanged between these two regions, the interface boundary condition must be given. This interface boundary condition can be treated in two different ways, in one hand it can be perfect contact interface (4), this assumes both temperature and heat flux continuity, and on the other hand a contact resistance (5) that assumes the existence of a temperature discontinuity at the interface. Based on the above, this interface boundary condition can be modelled mathematically by the following equations:

$$\left(T_p = T_c \right)_{\text{interface}} \tag{3}$$

$$k_c \left(\frac{\partial T_c}{\partial n} \right)_{\text{interface}} = -k_p \left(\frac{\partial T_p}{\partial n} \right)_{\text{interface}} \tag{4}$$

for the prefect contact interface,

$$k_c \left(\frac{\partial T_c}{\partial n}\right)_{\text{interface}} = -k_p \left(\frac{\partial T_p}{\partial n}\right)_{\text{interface}} = h_i \left(T_p - T_c\right)_{\text{interface}} \tag{5}$$

for the contact resistance interface. In these equations in terms of notation, h_i is the interface heat transfer coefficient and n is the interface normal vector.

The Equation (6) represents the energy equation used by the OF.

$$\frac{\partial \rho c_p T}{\partial t} + \nabla \cdot \left(\rho c_p \vec{u} T\right) - \frac{k}{\rho c_p} \nabla^2 T = 0 \tag{6}$$

This form of energy conservation equation contains the rate of change, advection and diffusion terms. Since the problem of interest is steady state, the rate of change term does not have to be considered, however it was used in the numerical calculations just for relaxation purposes, to facilitate the convergence. Accordingly all the results were considered when the calculations achieved steady state conditions. This was done by checking, in each time step, the initial and final residual values of the equation. When, for several time steps, these values were the same and do not changed, the steady state was assumed.

The Equations (1) and (2) are simplifications of Equation (6). For the polymer, Equation (1), the diffusion term is expanded for all directions and the advection term is only expanded for the z direction, since only the z velocity component is not null. In the case of the calibrator region, Equation (2), since it is stationary, the only term that subsists is the one that accounts for the contribution of heat diffusion.

Numerically all the governing equation terms have to be discretized. The schemes employed in this operation will have a direct influence on the order of convergence of the numerical code. The advection, diffusion and rate of change terms were discretized using, respectively, bounded Gauss upwind, Gauss linear uncorrected and Euler schemes. The schemes used to discretize both, the diffusion and advection terms, are second order, while for the rate of change is first order. However, since the

relevant results will be the ones of the steady state conditions, this first order scheme, will not influence the order of convergence for the developed code.

Another important subject regarding the numerical procedure is the type of boundaries and boundary conditions used on the model. Being the model composed by two different regions, polymer and calibrator, and the equations solved for each one of the regions, an interface between the two regions is part of it, meaning that a boundary has to be modelled to consider that interface.

In terms of the type of boundary used to model the interface between the regions, the *mappedWall* type was used. This type of boundary is used to couple two boundaries from two different regions, this means that the new boundary allows exchange of data between the regions, usually a field depending on the boundary condition used (OpenFOAM® Thermal modelling, 2014). This boundary type works by obtaining the values present on the interface boundary faces of the other region and use them on the calculations on its own region, creating a connection and allowing the exchange of energy, for example, between the regions.

Regarding the boundary condition applied on the interface between the regions, the *compressible::turbulentTemperatureCoupledBaffleMixed* condition was used. This boundary condition was designed to couple thermally solid and fluid regions, meaning that heat fluxes can be exchanged between both regions (OpenFOAM® Thermal modelling, 2014). It allows the user to introduce thermal layers on each side of the interface, each layer defined by its thickness and thermal conductivity, to create a contact resistance, see Eq. (5), between the regions. This boundary condition also allows to model the interface as perfect contact, see Eq. (4), if none thermal layer is defined. The properties of these layers are obtained using the relation $h = {k_l}/{t_l}$, where h is the contact resistance, k the thermal conductivity and t the thickness of the layer. The procedure to model an interface with a certain value for the contact resistance is the definition of the thickness by the user, and, using the previous relation, calculate the thermal conductivity. Subsequently, the values of thickness and thermal conductivity, are inserted at the interface boundary condition in both regions. On the boundary of each region used to thermally couple the regions, the same entries have to be used in each one of them, which creates two thermal layers with the same thickness and thermal conductivity.

Considering the model being developed in this project this boundary condition meets all the requirements to the construction of the interface between the polymer and calibrator.

2.4 Code Modifications Performed

Despite the fact of being a good choice to model the problem of interest, *chtMultiRegionFoam*, described on the section 2.2, it is not fully ready to be applied, some simplifications had to be performed on the *solver* source to solve only the required governing equations presented in Section 2.3. As illustrated on Fig. 2 on the fluid (polymer) region the *solver* calculates three different equations, while for the case of interest only the energy conservation equation has to be solved in this regions. In the polymer regions the velocity is known a priori and has a constant value.

The flowchart of the simplified solver is presented in Fig. 3.
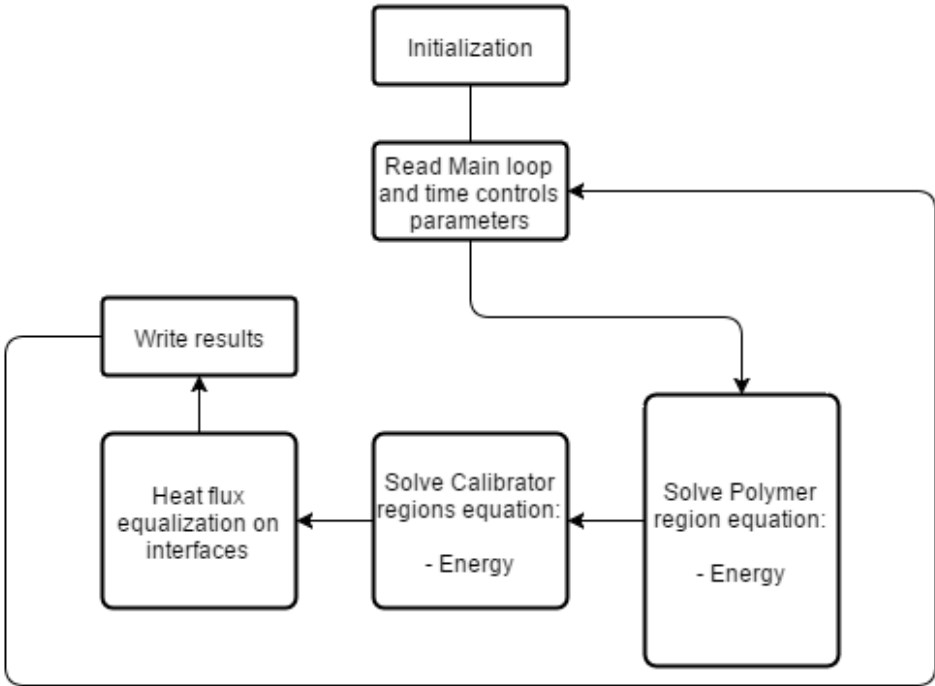
Fig. 3 - Flowchart of the modified solver steps

The flowchart of the new solver, illustrated on Fig. 3, is similar to the one illustrated by the Fig.2, although some changes were implemented. The step *Solve Fluid regions equations* is now smaller and the number of equations that are solved here was reduced. The momentum and continuity equations were removed from the source code, making the modified *solver* to use only the energy conservation when solving the equations for the polymer regions.

These simplifications were implemented on the original source code files, to create a new solver adequate to calculate the temperature distribution for the profile extrusion calibration/cooling stage.

3. NUMERICAL CODE VERIFICATION

In this chapter the previous developed code is going to be verified, which two problems comprising different complexity levels. The first verification consists of two stationary rectangular slabs that share a common face. The second verification consists in a more complex layout composed by a moving polymer sheet that is cooled by calibrator containing three transverse cooling channels.

3.1 Verification 1 – "Two Rectangular Slabs"

The two rectangular slabs case study, illustrated in Fig. 4. The two slabs made by different material share a common face. The boundary conditions used on the outer walls are fixed values of temperature, which is different in each slab.

The verification is going to be performed with comparison of the analytical solution for this problem, as described by Nóbrega J. M. et al. (2004), with the results for the temperature distribution obtained with the developed code considering the two possible interfaces, perfect contact and contact resistance. A convergence order study using several meshes, with different refinement levels, is also performed to evaluate the order of convergence of the developed code.

In terms of procedure, to obtain the geometries, this starts by being a single region which later is split into the desired two regions. This procedure is used due to the fact that the solver works with mesh regions and, to obtain these mesh regions, the entire geometry was constructed and meshed in a whole, which then was split into the different regions. The mesh used in this verification was obtained using *blockMesh* ("Mesh generation with blockMesh", 2015), a mesh generation utility supplied with OF. With this the mesh for the entire geometry was created and after, using the *topoSet* ("topoSet", 2012) utility, was divided into the S1 and S2 regions.

In terms of converge order study, this was performed with a mesh refinement ratio of 2, the error L-Infinty, L∞, which is defined as: $\|x\|_\infty = max_i|x_i|$ where x is difference between the numerical and the analytical value at the same location. The convergence order was calculated using $ord = \ln\left(\frac{error(Mi)}{error(Mi+1)}\right)/\ln\left(\frac{LM\_i+1}{LM\_i}\right)$, being LM_i and LM_i+1 the edge length of two meshes with different refinement degree, where i+1 refers to the mesh with smaller edge length.
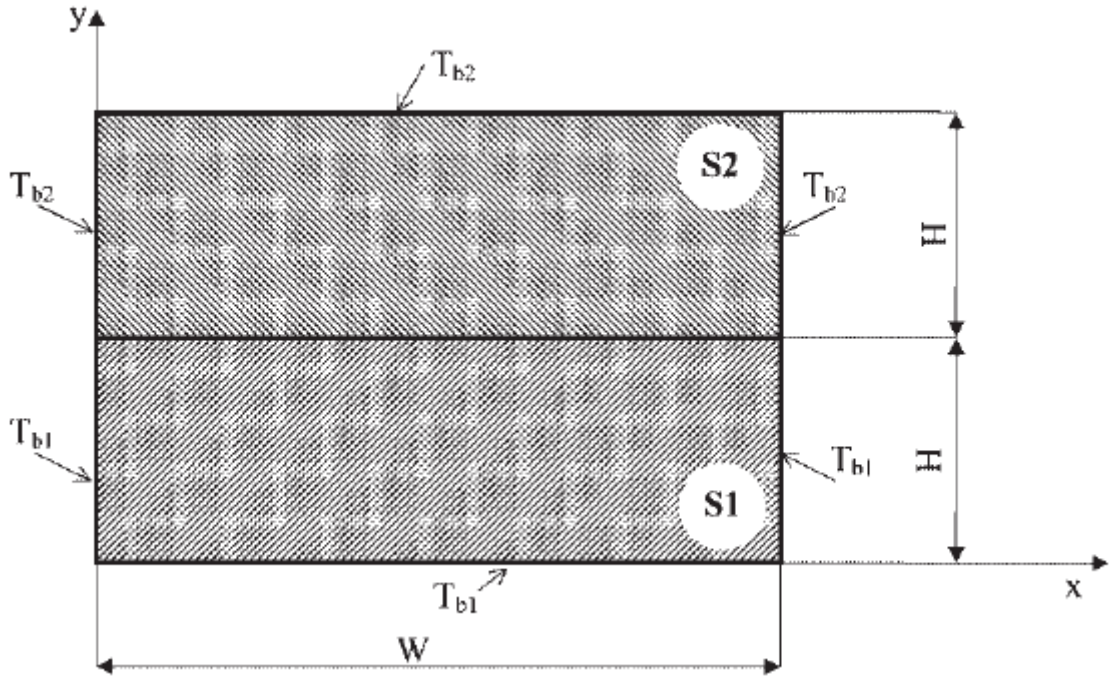
Fig. 4 – Verification 1 case study: geometry and boundary conditions, Nóbrega J. M. et al. (2004)

The analytical solution for this problem is given by Nóbrega J. M. et al. (2004) and for the case of perfect contact interface is given by:

$$T = T_{b1} + \sum_{n=1}^{\infty} \frac{2}{\pi}(T_{b2} - T_{b1})\frac{(-1)^{n+1}}{n}\frac{k_2}{(k_2 + k_1)}\sin\left(\frac{n\pi x}{W}\right)\sinh\left(\frac{n\pi y}{W}\right) \tag{6}$$

for the S1 region,

$$T = T_{b2} + \sum_{n=1}^{\infty} \frac{2}{\pi}(T_{b2} - T_{b1})\frac{(-1)^{n+1}+1}{n}\frac{k_1}{(k_2 + k_1)}\sin\left(\frac{n\pi x}{W}\right)\sinh\left(\frac{n\pi(-y + 2H)}{W}\right) \tag{7}$$

for S2 region.

For the contact resistance interface, the temperature distribution is given by:

$$T = T_{b1} + \sum_{n=1}^{\infty} \left[\frac{\frac{2}{\pi} h_i (T_{b1} - T_{b2}) \frac{(-1)^{n+1} + 1}{n} \times}{-k_1 \frac{n\pi}{W} \cosh\left(\frac{n\pi H}{W}\right) - \left(\frac{k_2 + k_1}{k_2}\right) \sinh\left(\frac{n\pi H}{W}\right)} \sin\left(\frac{n\pi x}{W}\right) \sinh\left(\frac{n\pi y}{W}\right) \right] \tag{8}$$

for the S1 region,

$$T = T_{b1} + \sum_{n=1}^{\infty} \left[\frac{\frac{2}{\pi} h_i (T_{b1} - T_{b2}) \frac{(-1)^{n+1} + 1}{n} \times}{k_2 \frac{n\pi}{W} \cosh\left(\frac{n\pi H}{W}\right) - \left(\frac{k_2 + k_1}{k_1}\right) \sinh\left(\frac{n\pi H}{W}\right)} \sin\left(\frac{n\pi x}{W}\right) \sinh\left(\frac{n\pi (-y + 2H)}{W}\right) \right] \tag{9}$$

for the S2 region.

3.1.1 Computational Model

The geometry, Fig. 4, used in this verification consists of two rectangular slabs, S1 and S2, with the same edge length and connected by a common interface. The dimensions used to construct this geometry were W = 100 mm and H = 50 mm. Regarding the properties used in each one of the slabs, the thermal conductivity for S1 and S2 is, respectively k_1 = 7 W/mK and k_2 = 14 W/mK. The boundary conditions used on the model are divided into two types, the fixed imposed temperature and the contact interface between the regions. For the temperature conditions on the S1 there is a fixed value, T_{b1} = 100°C, on the outer edges and for the S2 regions is also applied on the outer edges a fixed temperature value, T_{b2} = 180°C. As mentioned before, at the interface between the regions, two different conditions were tested, for a perfect contact interface and a contact resistance, with a heat transfer coefficient, h_i, of 500 W/m²K.
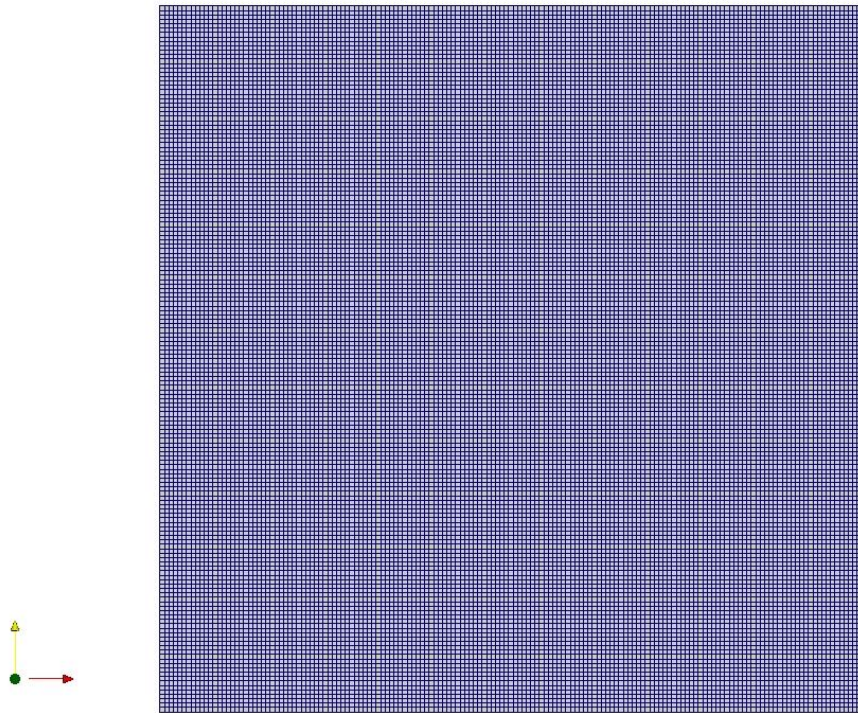
Fig. 5 – Verification 1 case study mesh M5

Regarding the mesh, illustrated by the Fig. 5, this is a structured mesh with 25600 hexahedral cells, with a minimum and maximum edge length of, respectively, 0,1 and 0,625 mm. Several meshes with different refinement degree are used in this verification and identified as M#, where M stands for mesh and # for a number from 1 to 5, being the 1 for the coarser mesh and higher the number also higher the refinement degree. These mesh refinement were obtained by dividing the maximum edge length by two. Starting by the M1 that has a maximum edge length of 10 mm and 100 cells, the M2 has a maximum edge length of 5 mm and 400 cells, the same procedure was applied for the remaining meshes. Regarding the number of cells for the remaining meshes, the M3 has 1600 and M4 has 6400 cells.

The results for the temperature distribution, with perfect contact and contact resistance interface, were obtained for several meshes using the developed code, to perform a comparison with the ones given by the analytical solution. For the temperature distribution at the line $x = 50$ mm, obtained with a perfect contact interface, illustrated in Fig. 6, it is noticeable that the temperature values obtained with the developed code, far from the interface, are coincident with the analytical ones, this even for the M1 which is the coarser mesh employed. Focusing on the interface, the values obtained with the analytical solution, at the same line, is 153.25°C for the bottom slab and 153.38°C for the top slab. Since it is modelled as perfect contact there should be no discontinuity on the temperature value at the interface, although, for the coarser meshes of the developed code results, a temperature discontinuity is predicted. This difference between the temperatures on each side of the interface gets smaller with the mesh refinements which means that the results are converging and by the M4 the discontinuity is practically inexistent and thermal continuity on the interface is almost achieved.

Fig. 6 – Analytical and numerical results for the temperature distribution of the Verification 1 case study: perfect contact

The convergence order values, Table 1, for the developed code show a good convergence of the results, when compared with the analytical ones. The order of convergence is close to second order,

which is expected, considering that the discretisation approaches employed (see Section 2.3) are second order as well.

Regarding the temperature distribution illustration in Fig. 7, considering that a perfect contact interface does not predict a temperature discontinuity between both regions, it shows, as expected, a continuous distribution at the interface.

Table 1 - Convergence order for perfect contact results of the Verification 1 case study

Mesh	Edge Length [mm]	Numerical Values		L∞ Error		Convergence order	
		S1 [ºC]	S2 [ºC]	S1 [ºC]	S2 [ºC]	S1	S2
M1	10	146.89	156.56	6.36	3.18	-	-
M2	5	150.17	154.92	3.08	1.54	1.91	1.91
M3	2.5	151.76	154.12	1.49	0.74	1.91	1.91
M4	1.25	152.54	153.72	0.71	0.35	1.85	1.82
M5	0.625	152.93	153.52	0.31	0.15	1.72	1.62
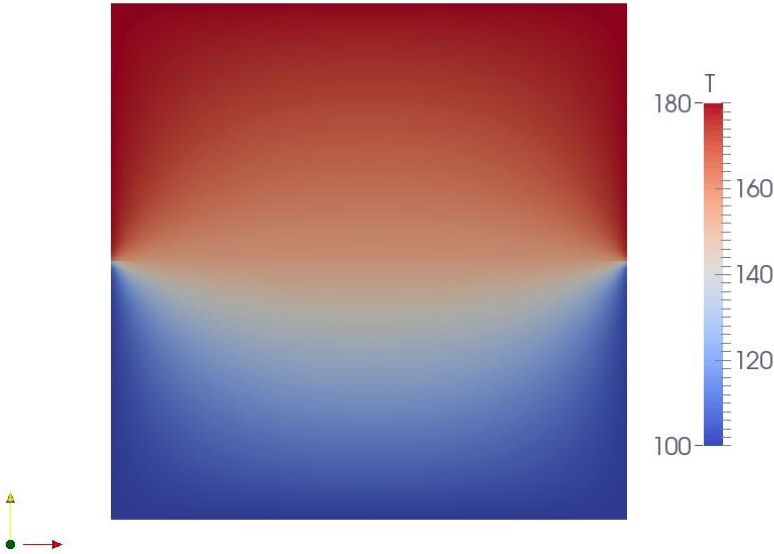
Fig. 7 – Temperature [ºC] distribution for the perfect contact interface, calculated by the developed code with M5

The results of the temperature distribution with the interface modelled with contact resistance, illustrated in Fig. 8, were obtained for several meshes on the line $x = 50$ mm across both slabs. Considering that, in this case, a contact resistance interface was employed, a temperature discontinuity

is expected to be obtained at the interface, which is shown by the analytical results where the values are 142.97°C and 158.51°C at the interface. Analysing the results on Fig. 8, as happened for the perfect contact case, the temperature values far from the interface are coincident with the analytical one. Although the values at the interface for the coarser meshes are considerably different from the analytical ones, the expected temperature discontinuity occurs at the interface. Setting the focus on the interface values, it is clear that the results obtained with the developed code converge to the analytical values with the mesh refinements. The results plotted on Table 2, show again a second order for the convergence, which is in accordance with the discretisation approaches employed for the governing equations terms, described in Section 2.3.
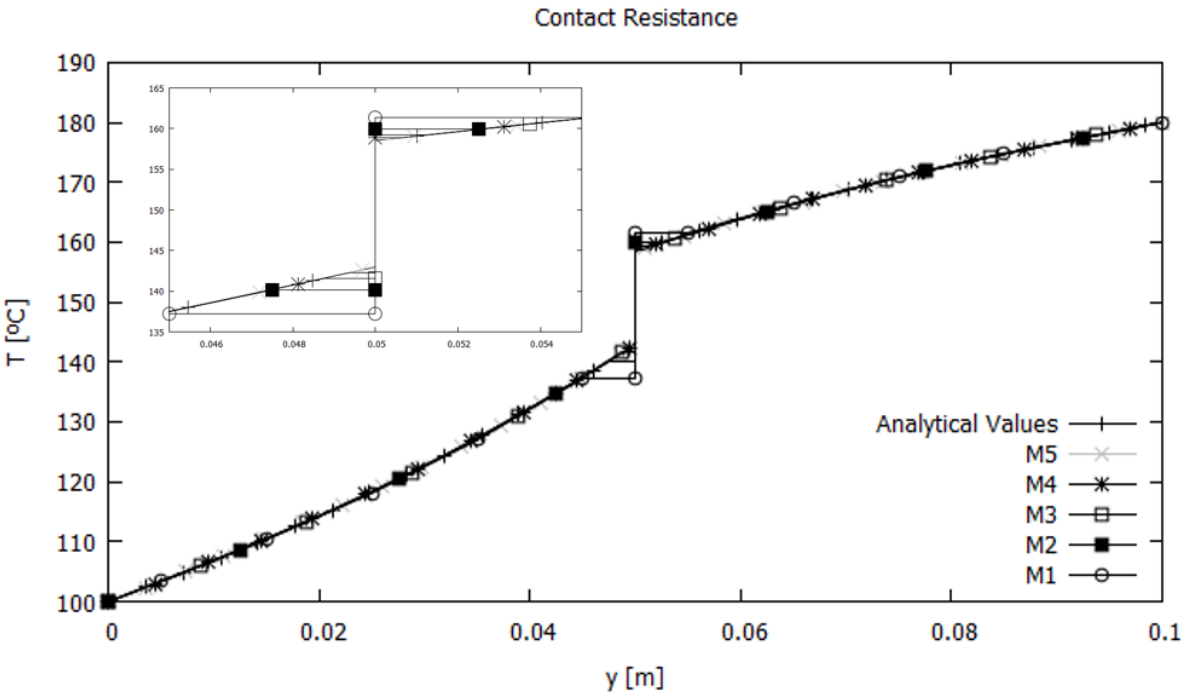
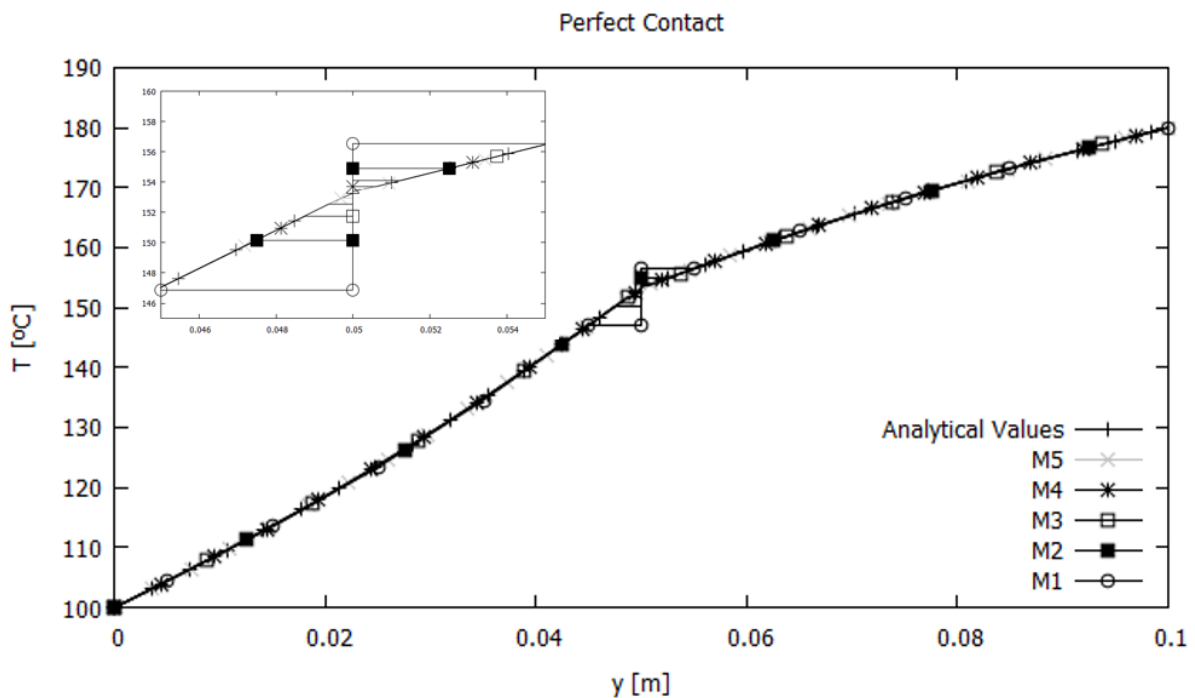*Fig. 8 – Analytical and numerical results for the temperature distribution of the Verification 1 case study: contact resistance*
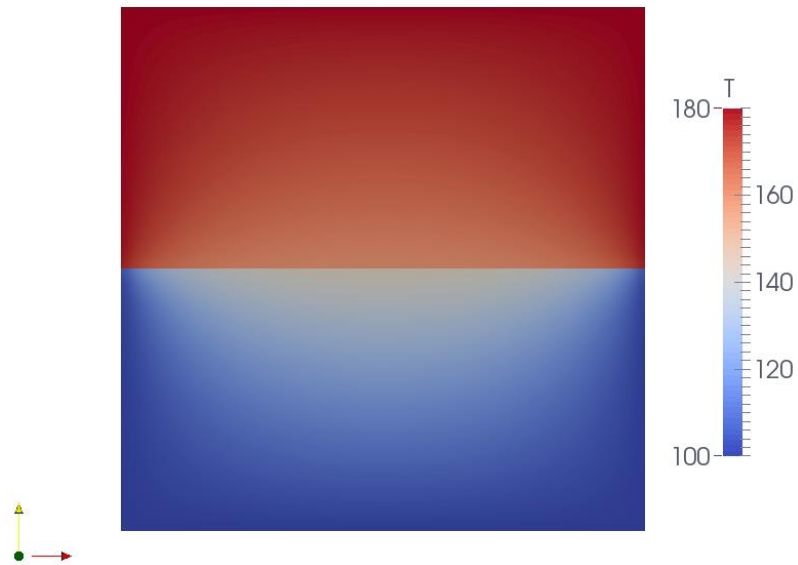
Fig. 9 – Temperature [ºC] distribution for the contact resistance interface, calculated by the developed code with M5

The temperature distribution, illustrated in Fig. 9, shows, as expected, a clearly defined temperature discontinuity between both regions.

The results obtained with both case studies presented in this sections, allowed to verify the developed code when diffusion is the only heat transfer process, since, in both cases, none of the domain parts is moving. The order of convergence was close to second order for both cases, as expected by the discretisation approaches employed to discretize the governing equation terms (see Section 2.3).

Table 2 - Convergence order for resistance contact results of the Verification 1 case study

Mesh	Edge Length [mm]	Numerical Values		L∞ Error		Convergence order	
		S1 [ºC]	S2 [ºC]	S1 [ºC]	S2 [ºC]	S1	S2
M1	10	137.20	161.40	5.77	2.88	-	-
M2	5	140.15	159.92	2.82	1.41	1.94	1.94
M3	2.5	141.57	159.21	1.40	0.70	1.97	1.98
M4	1.25	142.27	158.86	0.70	0.35	1.99	1.98
M5	0.625	142.62	158.69	0.35	0.17	2.00	1.97

3.2 Verification 2 – "Complex Layout"

A more complex problem is here developed to test the code for a more difficult and more similar model with the one being developed in this project. The temperature distribution obtained with the developed code are compared with the one given for the same model and available on the scientific literature, Nóbrega J. M. et al. (2004). This 2D layout is composed by a polymer sheet and a calibrator, as illustrated on Fig. 10. The polymer sheet is moving, at a constant and uniform velocity, while the calibrator is stationary. For this case, diffusion and advection transport mechanisms were considered, due to the fact that the polymer sheet is moving. Concerning the boundary conditions, the polymer sheet, has an inlet fixed temperature and, the calibrator, has a fixed temperature imposed on the cooling channels. A mesh convergence study was also performed to evaluate how the results behave with mesh refinement changes. For this study, six meshes, with different refinement levels, were used to obtain the temperature distribution in different locations with the developed code, the L2 error, defined as $|x| = \sqrt{\sum_{k=1}^{n} |x_k|^2}$, where x_k is the value of the difference between the result obtained and the reference one, was calculated and using number of cells of each mesh the convergence order was calculated, as described by S. Clain et al. (2013). Due to the fact that, for this case study, an analytical solution was not available, the L2 error was obtained using a reference value. This reference value was obtained by refining the mesh until no variations on the results was achieved and when subsequent mesh refinements obtained the same results, these were used as reference.
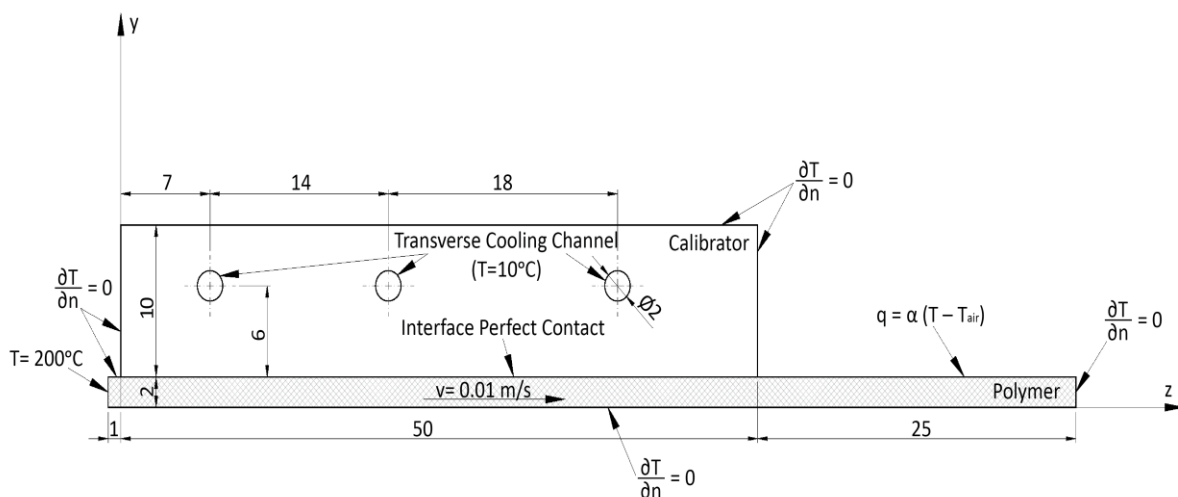

Fig. 10 - "Complex Layout" geometry and boundary conditions, dimensions in mm. Nóbrega J. M. et al. (2004)

3.2.1 Computational Model

The geometry of this model, Fig. 10, is 2D and composed by two different regions, the polymer and the calibrator. The polymer region is located at the bottom, has a total length of 76 mm and a thickness of 2 mm. This region is in contact with the calibrator on the total length of the later, which is 50 mm. The calibrator region has a 10 mm thickness, is located on top of the polymer region and contains three transverse cooling channels. These transverse cooling channels have a 2 mm diameter and they are located at 7, 21 and 39 mm distance from the left edge of the calibrator. This is a slightly modified version of the case study proposed by Sheehy et al. (1994), where the inlet location on the polymer region is slightly displaced to the left, where the original is aligned with the calibrator left edge. When using the Finite Element Method to discretize the governing equations, this alignment creates an unrealistic scenario, where the temperature gradient in direction normal to the interface is null, a direct consequence of assuming that the temperature of the calibrator next to the polymer is equal to the melt inlet temperature, as explained by Nóbrega J. M. et al. (2004).

Regarding the physical and thermal properties employed in each region of this model, as described by Sheehy et al. (1994), for the calibrator region the thermal conductivity was defined as k_c = 23 W/mK, on the other hand, for the polymer region, the thermal conductivity was defined as k_p = 0.18 W/mK, the density as ρ_p = 1400 kg/m³ and the heat capacity as c_p = 1000 J/kgK.

There are several boundaries that were used to model this verification, as illustrated on Fig. 10. For the polymer region a fixed inlet melt temperature of 200°C was used on the left side, the bottom edges, the end of the polymer section and the small edge between the inlet and the calibrator were defined as insulated. The top edge, on the last polymer section that is not in contact with the calibrator, is defined as free convection. Regarding the boundaries used on the calibrator region the outer edges were defined as insulated and the cooling channels have a fixed temperature of 10°C. To finish the modelling of this verification in terms of boundary conditions, the interface between the polymer and the calibrator region was modelled as perfect contact.

The mesh used to obtain the final results of this verification was constructed using *Salome* and the *Netgen* meshing algorithm. This is a mesh composed by triangular shape cells. Part of the M6 is illustrated on Fig. 11, this mesh has a total of 217914 cells and the minimum and maximum edge length is, respectively, 0.067 mm and 0.179 mm. Regarding the other meshes, used on the convergence study, the same procedure was used to obtain them (see Section 3.1.1). The number of cells for M1, M2, M3, M4 and M5 is, respectively, 298, 1016, 3380, 13520, 54698.
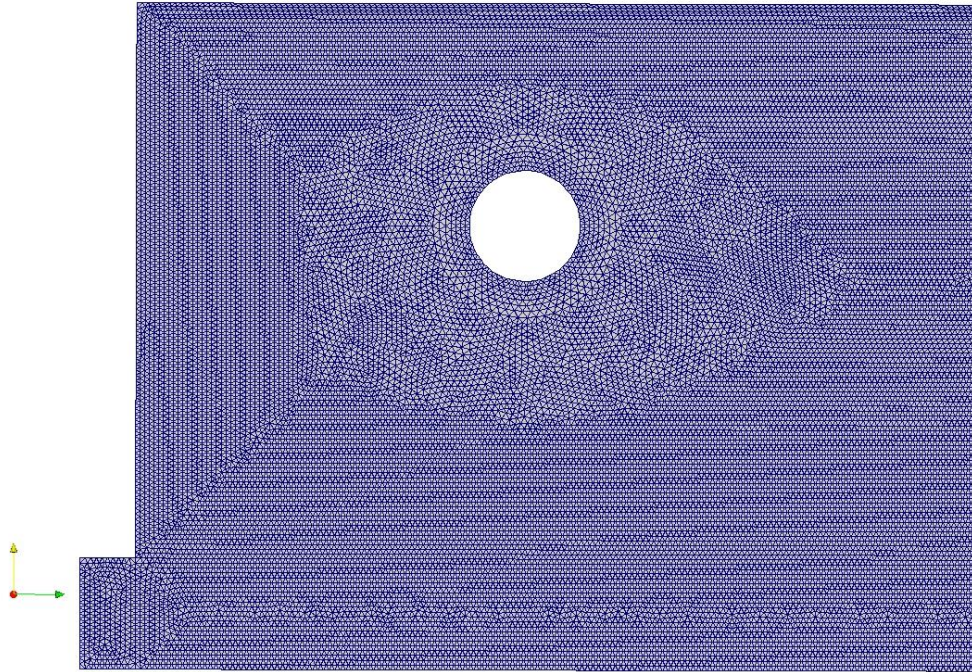
Fig. 11 – Verification 2 case study mesh M6

3.2.2   Results and Discussion

A convergence order study was conducted to evaluate the convergence of the results obtained with the six meshes described in the previous section. For this study the results were obtained on a line crossing both regions, polymer and calibrator, located at $z/L = 7/50$, illustrated in Fig. 12. The L2 errors and convergence order are shown on Table 3. Analysing the convergence order values for all locations, a close to second order value is achieved, which is expected considering the discretisation approaches employed (see Section 2.3). Bottom line for all locations a good agreement between the results is obtained with the M6, making it trustable to be use to obtain the final results.

	L2 Errors [ºC]			Convergence Order		
	z/L = 7/50	z/L = 30/50	z/L = 50/50	z/L = 7/50	z/L = 30/50	z/L = 50/50
Mesh_1	3217.55	2547.22	2840.61	-	-	-
Mesh_2	951.20	751.68	940.39	1.76	1.76	1.59
Mesh_3	275.70	191.65	224.67	1.79	1.97	2.07
Mesh_4	82.18	55.21	74.01	1.75	1.80	1.60
Mesh_5	20.34	15.63	21.74	2.01	1.82	1.77
Mesh_6	5.13	4.36	5.91	1.99	1.84	1.88
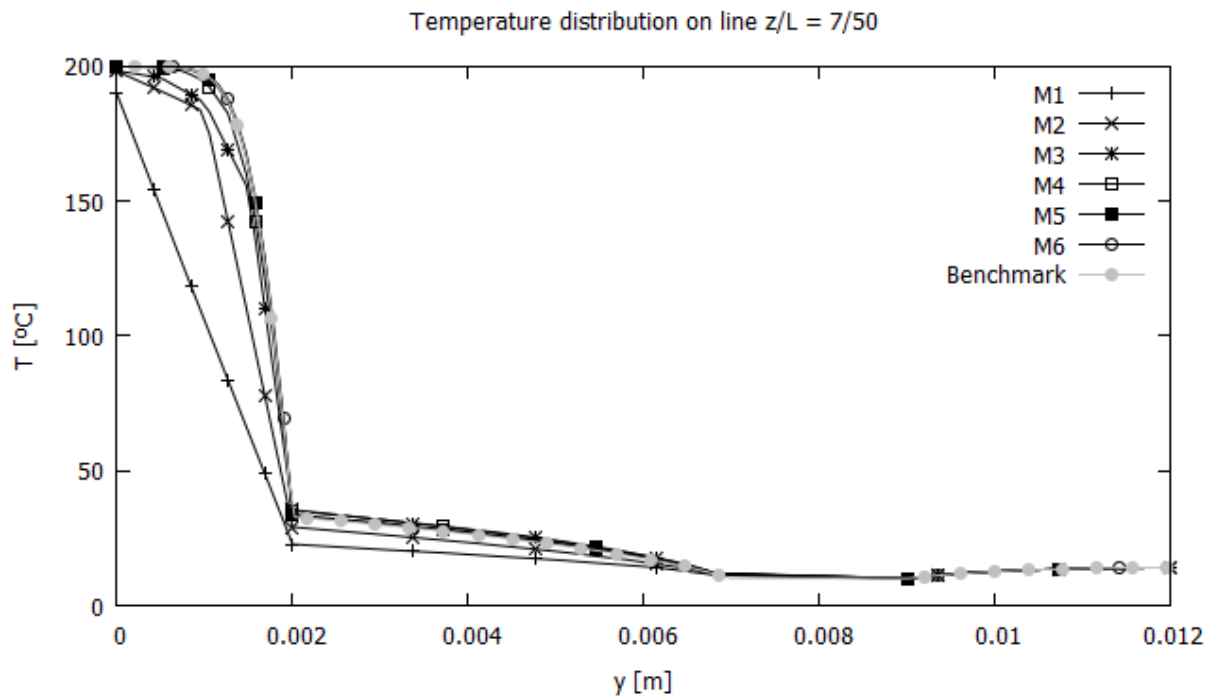
Fig. 12 - Results for several meshes on the location 7/50 of the complex layout, benchmark from Nóbrega J. M. et al. (2004)

The Fig. 12 also contains the results obtained by Nóbrega J. M. et al. (2004) for the same location allowing to understand how the results obtained with the developed code evolve with the mesh refinement. Analysing the results obtained with the developed code and compare them with the reference ones, M1 do not show a good agreement with the benchmark results. At this location, with M1, the temperature values decrease linearly throughout the polymer region and the temperature value on the interface is significantly different from the benchmark value. Although the model starts to show better agreement with

the M3 showing already a non-linear temperature decrease in the polymer region and the temperature value on the interface is closer to the benchmark one. The results obtained with M4, M5 and M6 are coincident with the benchmark values, showing a good agreement regarding the temperature distribution throughout both regions.

The temperature distribution, obtained using the developed code, across both polymer and calibrator regions is illustrated on Fig. 13. Four different locations were used to compare and analyse the results, retrieved by the developed code. These locations follow the same relation z/L and the locations used were 7/50, 30/50, 50/50, 75/50. The first location crosses the first cooling channel, the second one is approximately in the middle of the calibrator, the third is at the end of the calibrator region and, the last one, is at the end of the polymer region, this one only contain temperatures of the polymer section. The results were grouped in the Fig. 14 along with the reference results for the same locations.
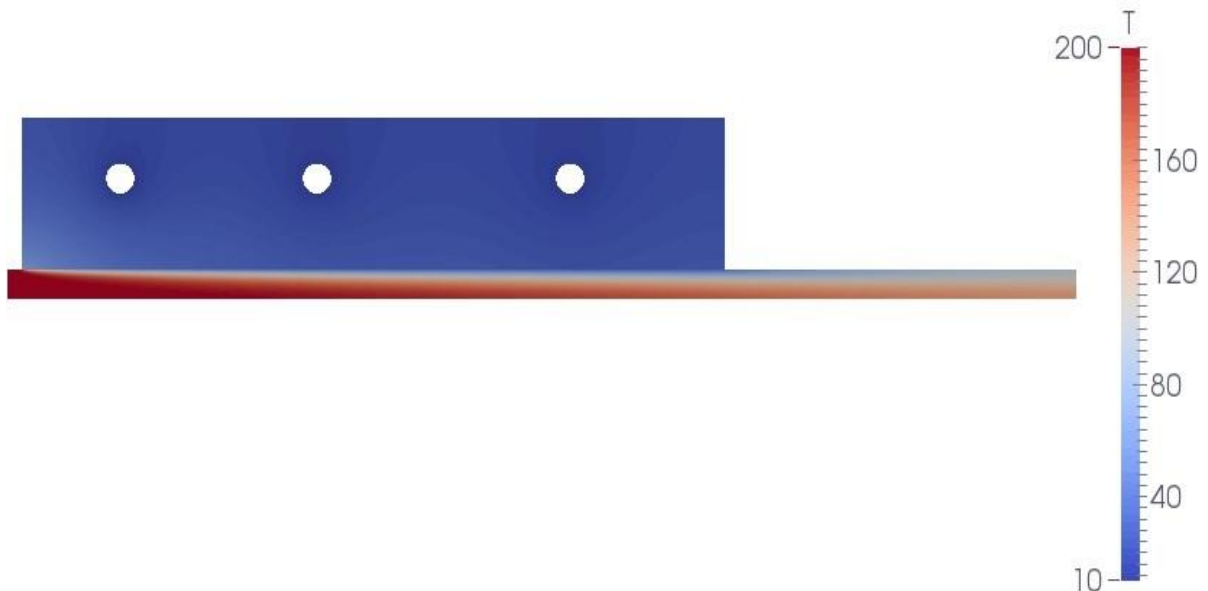
Fig. 13 - Temperature distribution illustration for the Verification 2, with M6

Analysing the results of the Fig. 14, it shows that the results obtained with the developed code are in agreement with the benchmark ones, except for the location 75/50 which is not in total agreement, this might happen due to the fact that the mesh used in this study was a lot more refined than the one used on the benchmark study. For the locations 7/50, 30/50 and 50/50 the agreement is clear throughout all temperature values. Moreover, the numerical results predict a continuous temperature distribution at the interface between the polymer and the calibrator, as expected, since the interface was modelled as perfect contact.
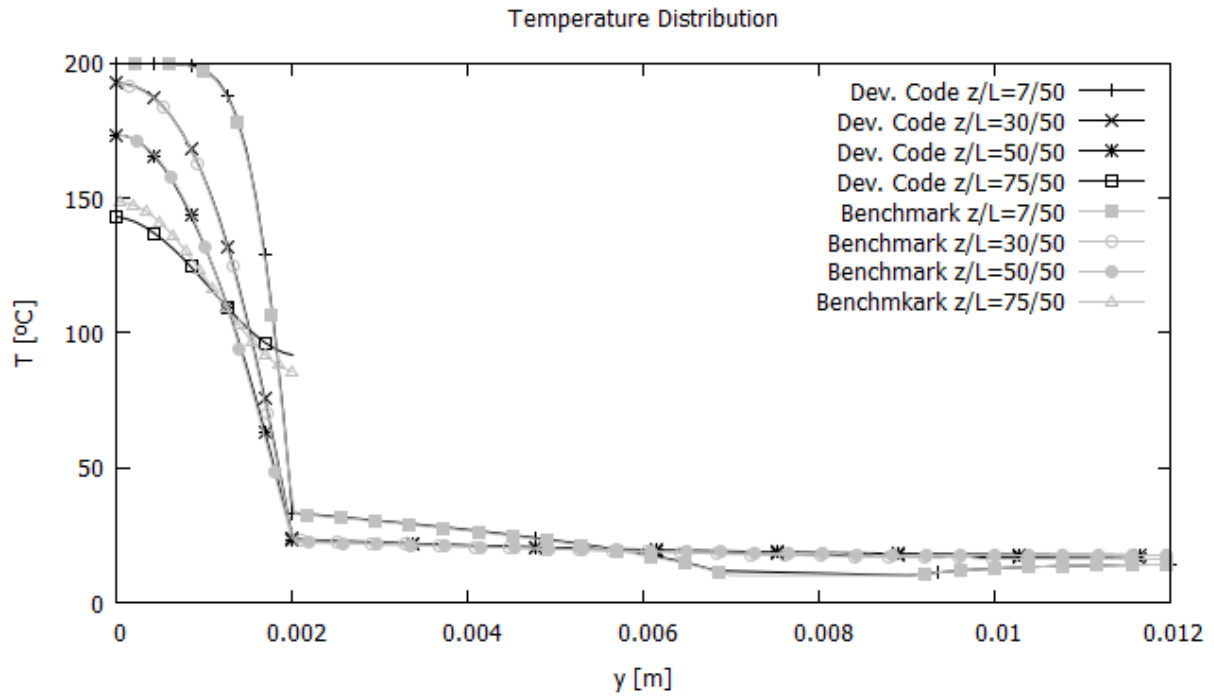
Fig. 14 - Temperature distribution for the Complex Layout case study, with M6. Benchmark from Nóbrega J. M. et al. (2004)

The developed code results, as stated, obtained a very good agreement when compared with the benchmark ones. This allows to conclude that the developed code is able to handle more complex layouts, even with moderately mesh refinements.

4. POLYMER CALIBRATION CASE STUDY

The numerical code, verified in Chapter 3, is now going to be used to study the cooling and calibration stage of the polymer extrusion process. The objective is to evaluate the influence of the boundary conditions, geometrical and process parameters on the performance of the cooling system. For this, three different studies were conducted, where two of them have the same process parameters employed although the layout polymer/calibrator is different between them and, the third one, different geometrical and process parameters were applied on the model and its influence, on the final results, is analysed. The same studies were conducted by Nóbrega, J. M. et al. (2004) and were used here to validate the numerical code developed in this work. These studies allow to evaluate the developed code capabilities in different geometries and under different conditions.

The cross section for all the following studies is shown in Fig. 15, except on the studies where the geometrical parameters of the calibrators are changed. This cross section is composed by a polymer part, on the inside, with a 70 mm x 60 mm rectangular outer contour and a 3 mm thickness, the calibrator part is positioned around the polymer with a 130 mm x 120 mm rectangular outer contour. This part also contains four transverse cooling channels with 8 mm of diameter and located at 12 mm from each profile cross-section edge. This is a simple cross section, although it is ideal to perform the first studies with a recently developed code.
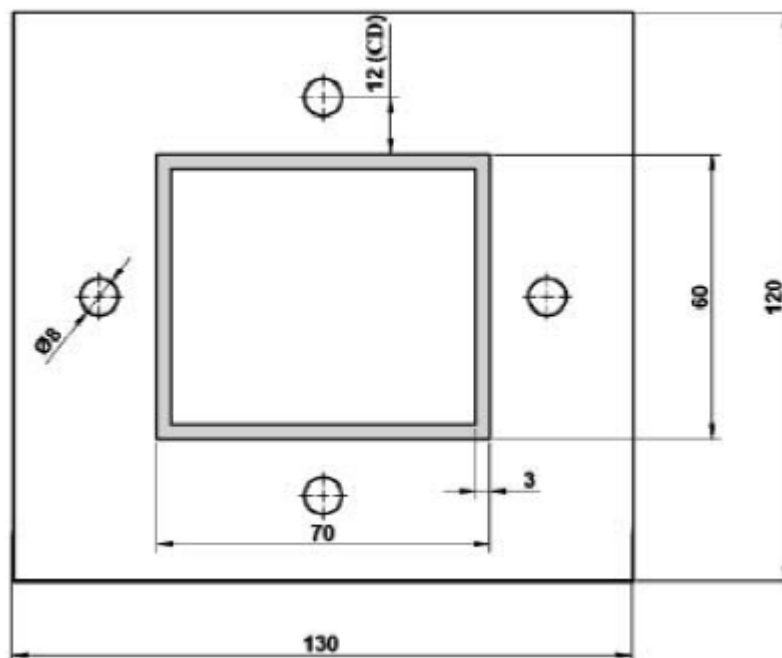
Fig. 15 - Polymer/calibrator cross section (dimensions in mm), Nóbrega J. M. et al. (2004)

The Table 4 describes the general/reference conditions and properties used in the studies.

Table 4 - Conditions and Properties used on the studies, Nóbrega J. M. et al. (2004)

Conditions and Properties Used	
k_p	0.18 W/mK
k_c	14.0 W/mK
ρ	1400 kg/m³
c_p	1000 J/kgK
Linear extrusion velocity	2 m/min
Inlet temperature	180°C
Room temperature	20°C
Cooling fluid temperature	18°C
Free convection heat transfer coefficient	5 W/m²K
Contact resistance heat transfer coefficient	500 W/m²K

The subscripts p and c stand for, respectively, polymer and calibrator. In terms of the conditions presented on the Table 4, the linear extrusion velocity is constant and applied only on the polymer region and the Inlet temperature is only applied on the profile inlet. The room temperature is a variable used when free convection at the outer walls is considered, on both polymer and calibrator regions, when this happens the free convection heat transfer coefficient is also used and both of these conditions are always constant. At the cooling channels walls a fixed and constant temperature of 18°C is considered. The table last entry is the heat transfer coefficient considered when modelling the interface between the polymer and the calibrator regions.

The Table 5 presents the different conditions, used on the model, for the different studies conducted. Two different types of conditions are considered, the boundary used at the outer walls of the polymer and calibrator regions and the heat transfer coefficient considered at the interface between the two regions. For the outer walls, two different cases are considered, the first is to use convection, which is having a heat flux leaving or entering the system through the outer walls, and the second is to consider the entire system insulated, meaning that no energy is lost through the outer walls. Another condition that could be considered on the outer walls is the radiation, although this condition has no effect on the results, as shown by Nóbrega J. M. et al. (2004), and was not considered in this work. Regarding the heat transfer coefficient used at the interface, three different values are going to be used, the perfect contact, which considers that there is no contact resistance at the interface, and the contact resistance with different thermal resistance. The code notation presented in Table 5 refers to an easier way to identify

the different cases solved, *c1* means that convection is used on the outer walls, *c0* means no convection, *h+* an increase of 50% on the heat transfer coefficient on the interface, *h-* a decrease of 50% on the heat transfer coefficient and *pc* stands for perfect contact.

Table 5 - Different conditions for outer surfaces and interface polymer/calibrator, Nóbrega J. M. et al. (2004)

Different Conditions Studied		
Code	Boundary for Outer Surfaces	Calibrator/Profile interface [W/m²K]
c1	Convection	500
c0	Adiabatic	500
h+	Convection	750
h-	Convection	250
pc	Convection	Perfect Contact

4.1 Three Calibrators Layout

This model is constructed using the previous shown cross section and it comprises using the polymer profile and three calibrators, with an annealing zone between each one of the calibrators, as illustrated in Fig. 16.

The developed code is going to be used to obtain the temperatures on the polymer profile cross section and the heat fluxes on the boundaries of the polymer and calibrators regions for the different cases on the Table 5.

The geometry of this model has four different parts, the polymer profile and three calibrators. The polymer profile has a total length of 850 mm and it cross section is the one described on Fig. 15, this part also has two annealing zones with 75 mm length when crossing from one calibrator to another. The three calibrators of the geometry keep the same cross section of the Fig. 15 and have a total length of 200 mm, they have a separation of 75 mm from each other and are in contact with the polymer profile on the inner walls across the total length of each of them.
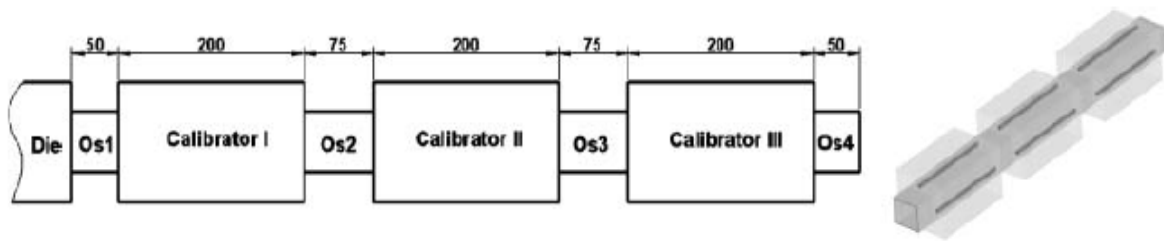
Fig. 16 - Geometry of the three calibrator layout (dimensions in mm), Nóbrega J. M. et al. (2004)

Each part of the geometry can be divided into different zones, for the polymer profile it is divided into the zones OS1, OS2, OS3, OS4 and one zone for each calibrator that it crosses. This is done to allow different boundary treatment in each of the zones. In terms of boundaries used in the zones OS1, OS2, OS3 and OS4, these will have two different states which are being insulated and considering convection on them. The zones when crossing the calibrators are considered as contact resistance, with the different heat transfer coefficients that are on the Table 5, and perfect contact, being these zones an interface between the polymer region and the calibrator regions. The inner walls of the polymer profile are always modelled as insulated. Regarding the boundaries used on the calibrators, the outer walls consider two situations, convection and insulation, the inner walls in contact with the polymer profile are modelled as contact resistance and perfect contact depending on the case being solved (Table 5) and the cooling channels that can be seen on the cross section (Fig. 15) have a fixed temperature condition, these are used in each one of the calibrators.

The Fig. 17 illustrate the mesh used to obtain the final results of this case study. This mesh was constructed using the *Salome* software and the *NetGen* meshing algorithm. The parameters were defined on the algorithm, retrieving a mesh, M5, with 39 million cells, all of them of the Tetrahedra type, with a minimum and maximum edge length of, respectively, 0.054 and 3.099 mm. Regarding the number of cells of the meshes used on the convergence study, M1, M2, M3, M4 have, respectively, 9972, 75492, 550731, 4591662.
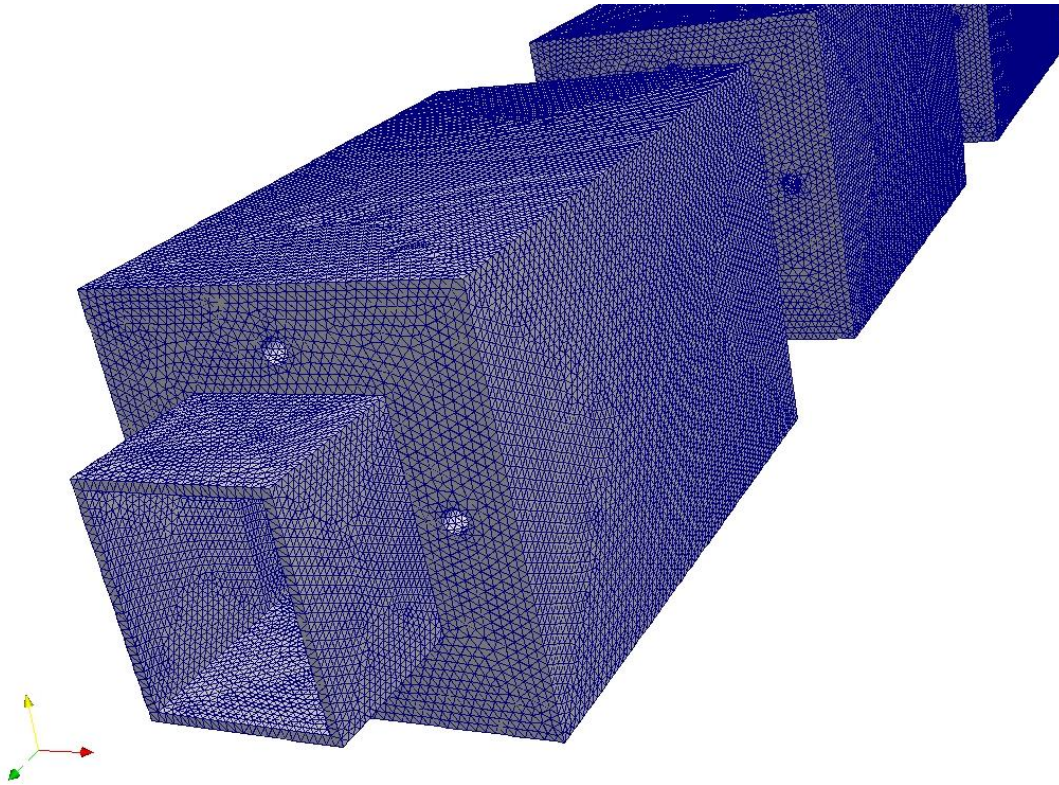
Fig. 17 – Three calibrator case study mesh

4.2 One Calibrator Layout

The second study performed using the developed code in presented in this section. In this case study the same cross section of the previous case is used, the layout, although, is composed with only one calibrator and the polymer profile, illustrated on Fig. 18. The developed code is going to be used to obtain the heat fluxes on the boundaries and temperatures at the end of the polymer profile cross section for the different studies shown on the Table 6.
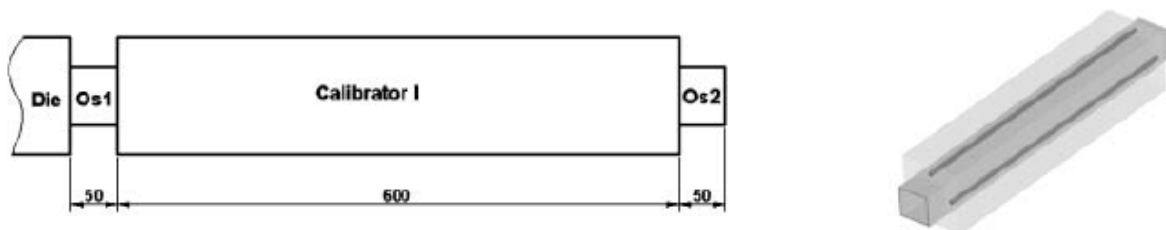
Fig. 18 - Geometry of the one calibrator layout (dimensions in mm), Nóbrega J. M. et al. (2004)

The geometry of this model is constructed with two parts, the calibrator and the polymer profile, both have the cross section of the Fig. 15. The polymer profile has a total length of 700 mm and has three different zones, the OS1, OS2 and the interior that is in contact with the calibrator, the first two are not in contact with any specified region and have a length of 50 mm each, the third has the same length of the calibrator. The calibrator has a total length of 600 mm, being in contact with the profile on the inner surfaces. In terms of boundary conditions used in each zone, regarding the polymer profile the OS1 and OS2 zones use convection or insulation and the contact established with the calibrator is perfect contact and contact resistance, with different heat transfer coefficients. On the calibrator the outer surfaces use convection or insulation, the interior surfaces in contact with the polymer profile use perfect contact and contact resistance with different heat transfer coefficients and the cooling channels use a fixed temperature of 18°C.

The mesh used in this study, illustrated in Fig. 19, was obtained using *Salome* and the *Netgen* algorithm, same as the previous case study. The same mesh refinement level obtained on the previous convergence study was using in this mesh, which retrieved a mesh with around 31 million cells of the Tetrahedra type, with a minimum and maximum edge length of, respectively, 0.0065 and 4.5898 mm.
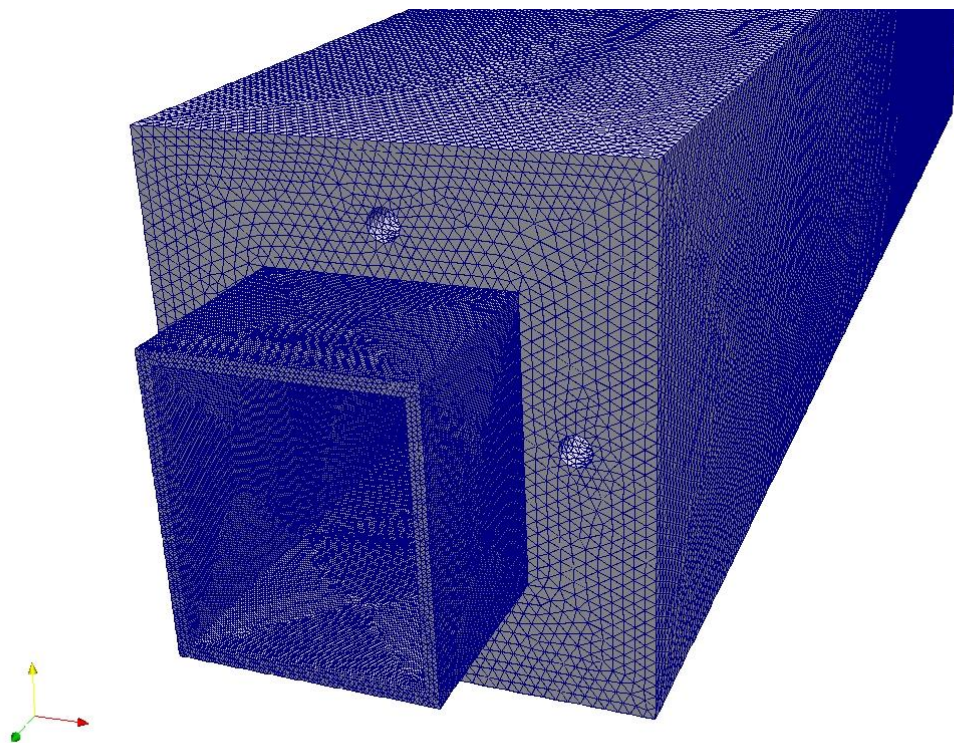
Fig. 19 - One calibrator case study mesh

4.3 Process and Geometrical Parameters

The previous case studies were used to evaluate the results behaviour when the boundary conditions on the outer surfaces and on the interface between the polymer and the calibrator were changed and also the number of calibrators, a geometrical parameter. This was also used to further assess the developed code, when tested with different boundary conditions, which performed qualitatively well on the several different cases solved.

The following case study uses, several more, process and geometrical parameters that can be changed in a real situation. The temperatures at the end of the cross section and the total heat removed from the polymer profile was obtained with the developed code. With this study, it is possible to identify how much the process parameters influence the final results, as well as the influence of the geometrical parameters. This also allows to choose the best parameters to apply on the cooling and calibration stage of the extrusion process.

To study the influence of the process and geometrical parameters, the one calibrator layout (see Section 4.2) was used with the conditions of the $c1$ case (see Table 5), except when a specific process parameter was changed. The parameters changed are shown on the Table 6. Regarding the process parameters, the cooling fluid that is present on the cooling channels of the calibrator is going to be used with two different temperature values, 12 and 24°C, as well as the profile velocity is going to be used with the values 1 m/min and 3 m/min. Considering that these values, on the $c1$ case, are 18°C and 2 m/min for cooling fluid temperature and profile velocity, respectively, a change of 50% above and below the reference values is applied.

The geometrical parameters are important in terms of the calibrator performance, some more than others, which this study is able to obtain enough data to identify how the parameters influence the performance. The first geometrical parameter considered was the number of calibrators used, which is similar to the three calibrator layout, where the total length of the one calibrator is divided by three calibrators and annealing zones are created between them. The second geometrical parameter is the position of the cooling channels on the calibrator, for the reference case they are at the middle of each side of the profile and here their location is changed to two different situation. The first moves, the four cooling channels, close to the corners of the profile, on the other hand, the second places two cooling channels next to each other, also meaning that the number of cooling channels is increased to eight. The last two geometrical parameters considered are the distance between the centre of the cooling channel and the profile surface, again with a value of 50% above and below the reference value. The other and

last parameter considered is the cooling channels diameter, changing its value to 50% above and below the reference case diameter.

Table 6 - Process and geometrical parameters used

	Code	Parameter	Description/Value
Process Parameters	**tw +**	Cooling Fluid Temperature	12°C
	tw -		24°C
	vp +	Profile Velocity	1 m/min
	vp -		3 m/min
Geometrical Parameters	**nc**	Number of Calibrators	Divide the total cooling length into three individual calibrators
	la	Cooling Channels Layout	Four cooling channels close to the profile's corners
	lb		Two cooling channels next to each other
	cd +	Distance between cooling channels and profile surface	8 mm
	cd -		16 mm
	dw +	Cooling channels diameter	4 mm
	dw -		12 mm

4.4 Mesh Sensitivity Study

A convergence order study was first performed to evaluate the convergence of the results when the mesh refinement degree is changed, it is expected to obtain results with a higher error with coarser meshes and this study also allows to identify what level of refinement should be used, to obtain trust worthy results for the model being studied. The procedure to obtain the convergence order is the one described by S. Clain et al. (2013) where the equation used was $ord = 2\ln\left(\frac{error(M1)}{error(M2)}\right)/\ln\left(\frac{M2}{M1}\right)$ where the factor 2 was changed to 3 since this is a 3D mesh. The error was calculated as the difference between the value of the total heat flux obtained with the developed code and the value obtained using the Richardson extrapolation method.

For every mesh the heat fluxes through the boundaries were calculated, using the developed code. Then the total heat flux removed from the system was used to calculate the order of convergence. The Table 7 shows the results and errors for each mesh, the mesh information and the convergence order using the case *c0*.

Table 7 - Results and convergence order for the three calibrator layout, case c0

c0	N.º Cells	Total Heat Flux [W]	Error [W]	Convergence Order
M1	9972	-2128.03	1245.47	--
M2	75492	-2180.93	1192.57	0.06
M3	550731	-2237.15	1136.35	0.07
M4	4591662	-2901.48	472.02	1.24
M5	39118817	-3336.37	37.13	3.56
Richardson Extrapolation	-3373.50			

Regarding the results it is clear that for the coarser meshes, that is M1, M2 and M3, the total heat flux result is far from the expected and the convergence for those mesh refinements is small, with values of 0.06 and 0.07. This means that, for this model, it is required at least a refinement level like the M4 one, to obtain good results. Analysing the results for M4, here a large difference from the M3 is obtained, which ends up with a higher and more desirable convergence order, although since the difference was quite considerable another mesh refinement was required. Regarding the last mesh, M5, the error is smaller when compared to the M4 one, as expected, obtaining a larger convergence order towards the expected value, which allows to consider that the M5 refinement level is adequate for this model.

4.5 Influence of the Boundary Conditions and Number of Calibrators

The results for the case studies of the Table 6 for the three calibrator layout, comparing the heat fluxes at the boundaries and the temperatures on the profile cross section, are summarized on the Table 8 and Table 9. To obtain these results the *wallHeatFlux* and the *patchAverage utilities* of OF were used, where the first calculates the heat fluxes through the boundaries and, the later, provides the average value of a certain field on a specific boundary. This allows to understand how much energy each calibrator removes from the polymer profile and also what quantity of that energy is absorbed by the cooling channels. It is also possible to quantify how much energy is lost through the outer walls, as well as how

much energy is removed from the polymer profile on the annealing zones. To analyse the results the *c1* case is going to be considered as reference.

Table 8 - Heat Fluxes [W] through boundaries of the three calibrator layout study

		Calibrator 1			Calibrator 2			Calibrator 3			
Code	OS 1	Surface	Cooling	OS 2	Surface	Cooling	OS 3	Surface	Cooling	OS 4	Total Heat Flux
c1	-10.3	-1445.6		-11.2	-1087.7		-8.2	-793.5		-3.9	-3360.4
		-15.4	-1430.2		-10.4	-1077.3		-7.3	-786.2		
c0	0.0	-1445.6		0.0	-1091.7		0.0	-799.1		0.0	-3336.4
		0.0	-1445.6		0.0	-1091.7		0.0	-799.1		
h+	-10.3	-1633.8		-10.7	-1176.2		-7.4	-816.5		-3.4	-3658.2
		-17.5	-1616.3		-11.3	-1164.9		-7.6	-808.9		
h-	-10.3	-1076.0		-12.3	-878.2		-9.8	-701.7		-5.2	-2693.5
		-11.3	-1064.7		-8.2	-870.0		-6.4	-695.3		
pc	-10.3	-2209.3		-9.0	-1363.7		-5.3	-798.5		-2.0	-4398.1
		-23.7	-2185.6		-13.3	-1350.4		-7.5	-791.0		

The reference case, illustrated in Fig. 20, which accounts convection at the outer boundaries, show losses of 10.3, 11.2, 8.2 and 3.9 on the profile outer surfaces OS1 through OS4, respectively, and losses of 1445.6, 1087.7, 793.5 in the three calibrators, mostly lost through the cooling channels. The Table 9 shows the maximum, minimum and average temperature at the cross section at the end of the cooling stage. Analysing the results on Table 8, it is clear that most of the heat removed from the profile occurs at the interface between the polymer and the calibrator and, on the calibrator, most of the heat is removed by the cooling channels. The values on Table 9 are little affected by considering convection at the outer surfaces of the polymer and calibrator, however the conditions used at the interface between the profile and the calibrator are very important, as can be seen by the changes on the total heat removed on the cases *h+*, *h-* and *pc*. Changing the heat transfer coefficient on the interface has the highest impact on the total heat remove and, consequently, on the temperatures obtained on the cross section at the end of the cooling stage. The type of boundary used at outer surfaces has a negligible impact on the total heat removed, since most of the cooling takes place via the cooling channels. Although, not considering convection at the outer surfaces is inadequate when detailed information of the temperature along the profile is required. All the variations on the temperatures, shown on Table 9, are in agreement with the variations on the total heat loss. The highest variations occurs when the heat resistance on the interface is changed, which makes this parameter the most influent on the thermal performance of the system.
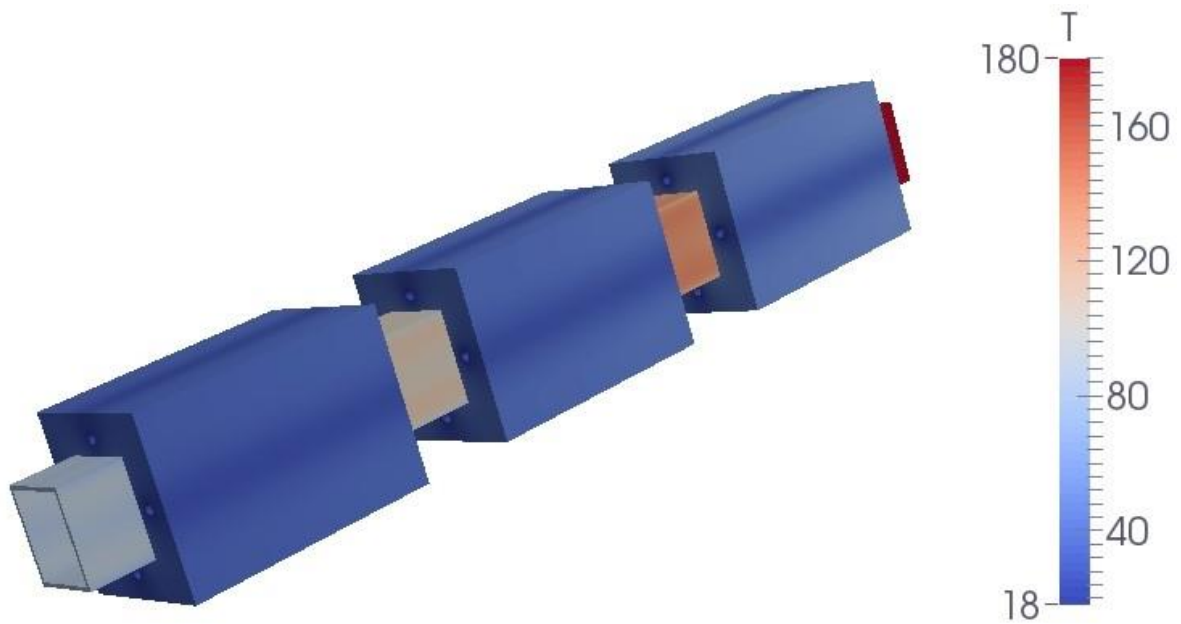
Fig. 20 - Temperature [ºC] distribution illustration for the three calibrator layout, reference case c1

A more detailed interpretation of the results of the Table 8, considering what is expected to occur when the conditions are changed, is conducted. For the reference case, *c1*, illustrated in Fig. 20, a small amount of energy is lost through the OS1 outer surface that increases when crossing the OS2 zone, which happens because of the length difference between these two zones. After that, the energy removed from the polymer profile on the OS3 and OS4 zones is smaller, as expected, since the temperature of the polymer should be lower after crossing two calibrators and, since convection depends on the temperature difference between the wall and the environment, a lower value is expected. Regarding the calibrators and starting from the distribution, the first calibrator is the one removing the highest amount of energy, which decreases on the second calibrator and on the third decreases even more. This is, obviously, expected since the polymer profile enters the first calibrator with higher temperature, which results in a higher heat flux passed to the calibrator. After that, the internal energy of the polymer decreases, which results on a smaller amount of energy transferred to the second calibrator and the same happens for the third one. The values on the outer surface of the polymer and calibrator should be considered, although the amount of energy removed in these areas is not large, when compared with the other values. Considering the results behaviour that can be predicted, such as the decrease of energy removed on subsequent calibrators, the heat fluxes obtained with the developed code, for this case, are in excellent agreement with the predictions. The *c0* case, where the outer surfaces are modelled as insulated, which means that through those surfaces no energy will cross, and so the system will not exchange energy with the outside. With this statement, a zero heat flux on the outer surfaces is expected and analysing the

results for this case, obtained with the developed code, this condition is fulfilled and zero energy is exchanged with the exterior. This means that the only way to remove energy from the system is through the cooling channels which the code takes in consideration. Comparing this case with the reference one, a decrease on the total heat flux is expected to be obtained and looking at the results it shows that a smaller amount of energy is removed, although the difference is not large, which shows that modelling convection on the outer surfaces has not a high impact on the final results. A higher heat flux value is found on the second and third calibrator, which is explained by the fact that, with annealing zones, the amount of internal energy on the polymer, when entering these calibrators, is higher than it is when there is convection on the outer surfaces. It is important to notice that the next cases use the same conditions on the outer surfaces as the *c1* case, which means that there is convection on both polymer and calibrator outer surfaces. The *h+* case has an increase on the heat transfer coefficient applied on the interface between the polymer and the calibrator. This change on the way the interface is modelled should create an increase on the energy exchanged from the polymer to the calibrator, since the thermal resistance on the interface is reduced with the increase of the heat transfer coefficient. This means that overall, since the conditions on the outer surfaces are the same as the one applied on the reference case, an increase on the total heat flux is expected to occur. Looking at the results, these behave as expected. An increase on the energy removed by all three calibrators is observed, keeping the expected variation when advancing from one calibrator to another. The OS1 value is the same of the reference case since that is no changes on that zone and on the OS2, OS3 and OS4 zones the results is smaller, since in each calibrator the amount of energy removed from the polymer profile is larger, resulting in less convection. The next case studied, *h-*, where the heat transfer coefficient on the interface is reduced to the minimum value used in these studies. This change means that there is a higher thermal resistance on the interface between the polymer and the calibrator, resulting in less energy transferred from the polymer profile to the calibrators. With this information, regarding the energy transferred on the interface in comparison to the reference case, it allows to predict that the amount of energy removed from the polymer profile is less than the reference case. Verifying the results it is noticeable that it varies as expected, meaning that the amount of energy removed per calibrator is smaller, also resulting in a total heat removed considerably smaller. Since less energy is removed in each calibrator, the OS2, OS3 and OS4 should get an increase on its values, because of the higher internal energy of the polymer profile while crossing these sections, this is also shown by the developed code results. The last case in this series, *pc*, is different from the reference case on the interface between the polymer and calibrators. This interface is modelled as perfect contact, resulting in an interface with infinite heat transfer coefficient, meaning that there is no thermal resistance

and that all the energy that reaches the interface is transferred to the other region, which the direction here is always from the polymer to the calibrator. With this analysis, the results expected to be obtained are a large increase on the heat removed from the polymer profile, in each one of the calibrators, and a large difference on the total heat removed, when compared to the reference case. Again, analysing the results obtained with the developed code, these show a clear increase on the heat flux on the calibrators, when compared with the reference case, which was the expected result concluded from the initial analysis.

Table 9 - Temperatures at the end of the profile cross section, three calibrator layout

Code		T min [ºC]	T max [ºC]	T average [ºC]
c1	Value	51.8	87.8	82.1
	Difference	-	-	-
c0	Value	54.2	88.5	82.8
	Difference	4.6%	0.8%	0.8%
h+	Value	43.9	79.9	73.5
	Difference	-15.3%	-9.0%	-10.5%
h-	Value	70.3	105.8	101.6
	Difference	35.7%	20.5%	23.7%
pc	Value	27.3	59.8	52.0
	Difference	-47.3%	-31.9%	-36.7%

The Table 10 shows the heat fluxes through the boundaries for the One Calibrator layout. For the reference case, *c1*, illustrated on Fig. 21, a small amount of energy is removed by convection on the polymer outer surfaces, OS1 and OS2, respectively 10.3 and 4.3. In agreement with the results on Table 8, for the Three Calibrator layout, most of heat is removed by the calibrator cooling channels. Table 11 contains the maximum, minimum and average temperatures of the cross section at the end of the cooling stage. Analysing the Table 10, it is clear that most of the heat is removed from the profile through its interface with the calibrator. Considering this, the values on Table 11, are little affected by the conditions used on the outer surface, which is clear by the small difference of the temperatures obtained for the *c0* when compared to the reference case. In contrast, the conditions used on the interface have the most impact on the total heat loss (case *h+*, *h-* and *pc*), which, consequently, have the most impact on the temperatures as well. For this layout, as happens for the previous one, the type of outer boundary has a negligible impact upon the total heat loss, mainly due to the fact that most of the cooling is performed by the cooling channels. Clearly, analysing the total heat loss and the temperatures, the most influent

parameter affecting the thermal performance of the system is the heat transfer coefficient, considered at the interface polymer/calibrator.

Table 10 - Heat Fluxes [W] through the boundaries for the table 5 cases, one calibrator layout

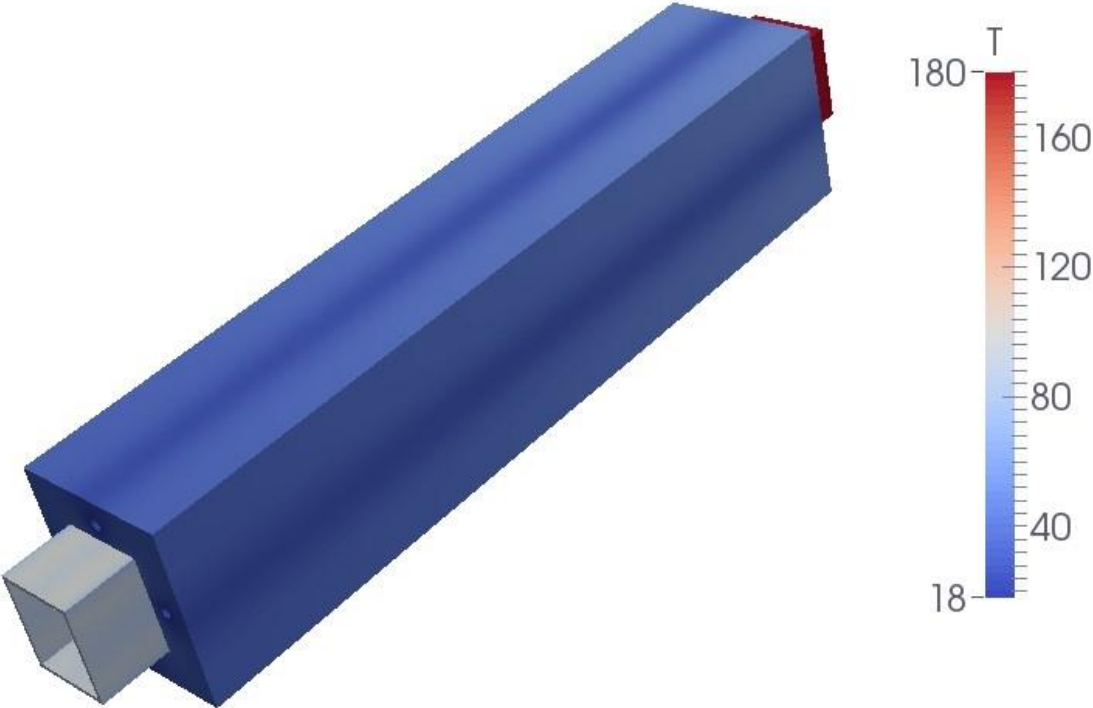| Code	OS 1	Calibrator		OS 2	Total
		Surface	Cooling		
c1		-3145.9			
	-10.3	-26.7	-3119.2	-4.3	-3160.5
c0		-3151.4			
	0	0	-3151.4	0	-3151.4
h+		-3414.5			
	-10.3	-29.1	-3385.3	-3.8	-3428.5
h-		-2534.8			
	-10.3	-21.0	-2513.8	-5.4	-2550.6
pc		-4087.2			
	-10.3	-35.4	-4051.8	-2.5	-4100.0

Fig. 21 - Temperature [ºC] distribution illustration for the one calibrator layout

The variations on the results of the Table 10, when the conditions are changed, follow the same line of the layout with three calibrators. This means that the variations on the results occur as expected and that, the changes on the conditions used, are correctly considered by the developed code.

Table 11 - *Temperatures at the end of the polymer profile cross section, one calibrator layout*

Code		T min [ºC]	T max [ºC]	T average [ºC]
c1	Value	48.3	93.9	87.6
	Difference	-	-	-
c0	Value	48.6	94.3	87.9
	Difference	0.62%	0.41%	0.37%
h+	Value	44.4	86.8	79.7
	Difference	-8.02%	-7.48%	-8.98%
h-	Value	60.1	110.0	105.5
	Difference	26.58%	18.62%	22.46%
pc	Value	27.4	69.1	59.7
	Difference	-34.78%	-22.55%	-26.42%

The two different layouts results are in good agreement between each other, regarding that, the changes applied on the boundary conditions, retrieved the same variations on the total heat lost and temperatures for both layouts. On both was clear that the heat transfer coefficient, used at the interface polymer/calibrator, is the most important parameter, in terms of performance of the cooling system. It was also clear that the impact of the type of boundaries used on the outer surfaces of the model is not relevant. A comparison between them show that it is more efficient to use three calibrator instead of one. On all the studies performed with both layouts, the total heat lost when using three calibrator was higher than when using one calibrator. Regarding the temperatures, a lower value of average temperature is obtained for the three calibrator layout, on all the studies. This is related with the effect of having annealing zones on the profile, which allows the heat to travel from the bulk to the surface of the profile, leading to a more homogenous temperature distribution.

4.6 Effects of the Geometrical and Process Parameters

The Table 12 presents the results of the studies conducted to evaluate the influence of process and geometrical parameters. In order to analyse the results, the *c1* case of the One Calibrator layout is taken as reference. The changes on the cooling fluid temperature (*tw*) has an effect considerably smaller than changes on the profile velocity (*vp*). Reducing the temperature of the cooling fluid a higher amount of heat is removed from the profile and lower temperatures are obtained, on the other hand, there is an increase of these values when the temperature of the cooling fluid is increase. The profile velocity is clearly more influent on the cooling performance, the differences on the temperatures and total heat removed are substantial. However, the advantages, on the cooling performance, obtained by reducing the profile velocity has the counter effect of reducing the production rate, which is not desired on the extrusion process.

In the case of the geometrical parameters, the difference on the results, when the distance of the cooling channels to the profile surface (*cd*) is changed, are not significant. In fact, increasing the distance (*cd +*) reduces the cooling efficiency, while reducing it produces at small increase on the cooling performance. The same analysis applies for the changes on the diameter of the cooling channels (*dw*), where the changes on the results are unimportant.

The use of four cooling channels close to the profile's corners (*la*) reduces the system cooling efficiency, although, the T_{min} is lower but T_{max} is higher. This creates a less uniform cooling of the profile, where the profile corners cool more efficiently than the middle. This is not an advantage for the profile cooling and this change does not promote any improvements.

Dividing the total cooling length into three individual calibrators (*nc*) promotes an increase on the total heat removed and a reduction on the average temperature obtained. The space between the calibrators promotes a reduction of the heat flux on the profile surface, which increases the temperature homogeneity on the profile, leading to a higher surface temperature and increasing the effectiveness of the subsequent cooling. To conduct a better analysis in order to conclude what parameters are more important to the process, a deeper interpretation of the Table 12 is required.

Table 12 - Temperatures and total heat removed for the process and geometrical parameters studies

	Code	T min [ºC]	T max [ºC]	T average [ºC]	Total Heat Removed [W]
Process Parameters	tw +	53.1	97.0	91.0	3058.8
	tw -	43.6	90.8	84.3	3290.7
	vp +	59.6	116.0	110.0	2248.7
	vp -	31.3	54.8	50.5	3648.0
Geometrical Parameters	nc	51.8	87.8	82.1	3360.4
	la	43.0	105.5	95.3	2911.6
	lb	39.6	87.1	81.6	3382.2
	cd -	47.3	931	86.1	3228.0
	cd +	49.9	95.6	90.5	3077.9
	dw +	45.5	91.0	85.0	3266.7
	dw -	54.7	99.5	93.7	2968.0

Starting by the *tw +* study, it is expected to obtain higher temperature at the end of the polymer profile cross section and, consequently, less total heat removed from the profile. This is related to the fact that, having the cooling fluid with higher temperature, leads to a lower amount of energy removed from the calibrator by the cooling fluid, since, from the start, the internal energy of the fluid, with increased temperature, is larger. Regarding this analysis, looking at the results, it is clear that the developed obtained results that follow the expectations, with a reduced total heat removed and higher temperatures than the reference case. The same analysis can be applied to the next case, *tw -*, although the expected result to be obtained with a lower cooling fluid temperature are lower temperatures and larger total heat removed, since the internal energy of the fluid, with lower temperature, is lower as well, allowing a larger amount of energy removed from the calibrator. For this case the results are the expected, obtaining lower values of temperature at the end of the polymer cross section and, consequently, a higher amount of total heat removed. Changing the cooling fluid temperature is possible, in a real situation, although changing this process parameter alters the cooling of the polymer. Continuing on the process parameters, the following two cases are solved with a different profile velocity. The main result of changing this process parameter, related with heat transfer, is the time that the polymer profile stays inside the calibrator. A larger amount of time spent by the profile inside the calibrator, means that more time is available to exchange energy between them both. This results in an expected result of considerably lower amount of total heat removed when the time spent on the calibrator is lower, which is the case with higher profile velocity, and a higher amount of total heat removed when the time spent inside the calibrator is larger, which is the case with lower profile velocity. The developed code obtained a significantly lower total heat

removed, when the profile velocity was bigger. Regarding the temperatures, as the total heat removed is smaller, the temperatures are higher than the reference case. For the case where the profile velocity is lower, vp -, a significantly higher amount of total heat removed was obtained with, consequently, lower temperatures at the end of the polymer profile cross section. On both of these cases, the results behave as expected when compared to the reference case, also allowing to understand that, the profile velocity, has a large impact on the final results.

The geometrical parameters considered in this case study are parameters that can be changed or selected during the design/development of the cooling and calibration stage of the extrusion process. The first case considered, nc, splits the calibrator into three individual ones that together have the same length of the first one. This also results into the appearance of annealing zones that help on the cooling of the polymer profile. Having three different calibrators, these are independent from each other and the cooling system is also independent which works in favour of cooling the profile. The results show that changing the number of calibrator within the same length range benefits the cooling of the profile, obtaining a higher amount of total heat removed and lower temperatures at the end of the polymer profile.

The layout of the cooling channels is another geometrical parameter that can be changed during the development of this stage, the influence they have on the final results is going to be analysed here. On the first cooling channels layout change, la, the location of the channels was changed to a position closer to the profile corners. This will reduce the area of the profile exposed to the cooling channel within a small distance, this means that the energy travel distance, from the profile to the cooling channel, is increased, except for the profile corners. With this distance increase the total heat removed should decrease and consequently the temperatures should increase. Looking at the results, the total heat removed follows the prediction, decreasing in comparison to the reference case, the maximum and average temperatures increase, although the minimum temperature decrease when compared to the reference case. This happens due to the fact that with the cooling channels in the current position, it creates a lesser uniform cooling of the profile, this way it has zones with low temperatures and zones with considerably higher temperatures, as well as creating a larger gap between the minimum and the maximum temperature. The last case regarding changes on the cooling channels layout, places two cooling channels next to each other on each side of the polymer profile. With the addition of a cooling channel on each side of the polymer, it is expected to be obtained a higher total heat removed and, consequently, lower temperatures. The results show an increase of the total heat removed and, regarding the temperatures, a considerably decrease on the minimum temperature and a smaller decrease on the maximum and average temperatures. The next geometrical parameter changed is the distance between

the profile surface and the centre of the cooling channels. Analysing both cases the expected results variation, when changing this parameter, is the more the distance is increased the less heat is removed and the less the distance, higher the amount of total heat removed. Looking at the results this correlation is confirmed, removing less heat when the distance is increased and more heat when the distance is reduced, although the difference between these cases and the reference one is not very large making this a parameters have a relatively lower influence on the final results. The last geometrical parameter to be studied is the diameter of the cooling channels, this change should work as: the larger the diameter, larger the total heat removed and: the lower the diameter, less total heat removed. Watching the results, it is noticeable that they correctly behaves having into account the previous analysis, showing an increase of the total heat removed, when the diameter is increased, and a reduced total heat removed, when the diameter is reduced. Regarding the temperatures, they also behave correctly, reducing when the diameter is increased and increase when the diameter is reduced. With all this information is possible to identify that the geometrical parameter with the most influence on the final results was the number of calibrators, obtaining a large amount of total heat removed with a more uniform temperatures. Regarding the process parameter it is clear that the profile velocity has the biggest impact on the final results, although this influence the production rate making it a sensible parameter to work with. Considering the average temperature and total heat removed, it can be concluded that splitting the cooling length into three calibrator has a performance similar to the *Ib* layout, which has a double number of cooling channels.

5. Conclusions and Outlook

5.1 Conclusions

The main objective of this project was the development of numerical tools adequate to model the cooling and calibration stage of the extrusion process, using unstructured meshes. This new code is able to solve the energy conservation equation on different regions, accounting for the heat exchange between them, which, considering the cooling and calibration stage, suits all the modelling requirements. Using the OF as a base to develop such tools, the process to achieve it was considerably facilitated. Which evidences that OF is an excellent tool to use when specific numerical tools have to be created to fulfil specific modelling requirements.

The developed numerical code, used in this project, was obtained by simplifying an existent OF solver. The new code was verified with two case studies. The first one consisted on the prediction of the temperature distribution across two slabs, with different properties and a common face, where only diffusion was considered as transport mechanism. The second one consisted on predicting the temperature distribution on a system composed by a polymer sheet and a metal calibrator, which, since the polymer sheet was moving, the diffusion and advection transport mechanisms were considered.

With the code verified, a case study, comprising three different studies, were performed. The first two studies intended to evaluate the results behaviour when different conditions are applied to the model, namely perfect contact and contact resistance on the interface between regions. The heat fluxes through the boundaries and temperatures at the end of the profile cross section were evaluated, where the developed code correctly handled the changes on the conditions used. These studies made possible to conclude that the developed code can handle different boundary conditions and also that the contact resistance has the highest impact on the results. The third case study was more focused on the parameters that can be changed or controlled in a real situation, which are the process and geometrical parameters. Here it can be concluded that the developed code correctly works when the process and geometrical parameters are changed, the results show a correct behaviour in each specific situation and also made possible to analyse that the profile velocity the most important process parameter, in terms of energy removed from the polymer profile. Regarding the geometrical parameter, it can be conclude that the number of calibrators/cooling units is the most important parameters. Despite not being the layout with the most amount of energy removed from the polymer profile, it obtains a more uniform temperature distribution, which is also important for the process.

All the studies performed allowed to conclude that the developed code is able to model accurately the cooling and calibration stage of the extrusion process, being able to cope with complex geometries.

5.2 Outlook

Considering that good results were obtained using the developed code on the cooling and calibration stage of the extrusion process, the author suggest that the following studies should be conducted:

Test the developed code with more complex cross sections, which can also include the creation of an adequate mesh generator to facilitate the expansion of the studies conducted.

An interesting approach would also be the coupling of this developed code with optimisation tools, targeting the automatic adjustment of geometrical and processing parameters in order to obtain the best conditions for a specific case.

Develop a tool able to calculate the temperature distribution standard deviation, on a specific area. A modification on the patchAverage utility is suggested, such modifications should include the implementation of the necessary routine to obtain the temperature distribution standard deviation.

REFERENCES

Carneiro, O. S., Nóbrega, J. M., Mota, a. R., & Silva, C. (2013). Prototype and methodology for the characterization of the polymer-calibrator interface heat transfer coefficient. *Polymer Testing*, *32*(6), 1154–1161.

Clain, S., Machado, G. J., Nóbrega, J. M., & Pereira, R. M. S. (2013). A sixth-order finite volume method for multidomain convection–diffusion problem with discontinuous coefficients. *Computer Methods in Applied Mechanics and Engineering*, *267*, 43–64.

Menges, G., Kalwa, M., & Schmidt, J. (1987). *Kunststoffe-German Plastics*, 77(8), 797.

Mousseau, P., Delaunay, D., & Lefèvre, N. (2009). Analysis of the heat transfer in PVC profiles during the extrusion calibration/cooling step. *Int. Polym. Proc.* 24(2), 122.

Nóbrega, J. M., Carneiro, O. S., Covas, J. a., Pinho, F. T., & Oliveira, P. J. (2004). Design of calibrators for extruded profiles. Part I: Modeling the thermal interchanges. *Polymer Engineering and Science*, *44*(12), 2216–2228.

Nóbrega, J. M. (2004). *Computer Aided Design of Forming Tools for the Production of Thermoplastic Profiles*, PhD thesis. Department of Polymer Engineering, University of Minho, Guimarães, Portugal.

Pittman, J. F. T., Whitham, G. P. (1994). Cooling and wall thickness uniformity in plastic pipe manufacture. *Int. Polym. Proc.* 9(2), 130.

Sheehy, P., Tanguy, P. A., & Blouin, D. (1994). *Polym. Eng. Sci.* 34, 650.

OpenFOAM® Thermal modelling (2014, February 17). Retrieved from http://www.openfoam.org/version2.3.0/thermal.php

Mesh generation with blockMesh. (2015, March 1). Retrieved from http://cfd.direct/openfoam/user-guide/blockmesh/

TopoSet (2012). Retrieved from https://openfoamwiki.net/index.php/TopoSet